Aneeka Zaheen Kamal

SYNTHESIS AND CHARACTERIZATION OF SINGLE-ION CONDUCTING POLYMER ELECTROLYTES FOR LITHIUM-ION BATTERIES

M.S.
2015

FATİH UNIVERSITY

The Graduate School of Sciences and Engineering

Master of Science in
Chemistry

SYNTHESIS AND CHARACTERIZATION OF SINGLE-ION CONDUCTING POLYMER ELECTROLYTES FOR LITHIUM-ION BATTERIES

by

Aneeka Zaheen Kamal

June 2015

SYNTHESIS AND CHARACTERIZATION OF SINGLE-ION CONDUCTING POLYMER ELECTROLYTES FOR LITHIUM-ION BATTERIES

By

Aneeka Zaheen Kamal

A thesis submitted to

The Graduate School of Sciences and Engineering

of

Fatih University

in partial fulfillment of the requirements for the degree of

Master of Science

in

Chemistry

June 2015
Istanbul, Turkey

APPROVAL PAGE

This is to certify that I have read this thesis written by Aneeka Zaheen Kamal and that in my opinion it is fully adequate, in scope and quality, as a thesis for the degree of Master of Science in Chemistry.

_____

Assoc. Prof. Sevim ÜNÜGÜR ÇELİK
Thesis Supervisor

I certify that this thesis satisfies all the requirements as a thesis for the degree of Master of Science in Chemistry.

_____

Prof. Abdulhadi BAYKAL
Head of Department

Examining Committee Members

Assoc. Prof. Sevim ÜNÜGÜR ÇELİK _____

Assit. Prof. Ayşe ASLAN _____

Assoc. Prof. Mehmet ŞENEL _____

It is approved that this thesis has been written in compliance with the formatting rules laid down by the Graduate School of Sciences and Engineering.

_____

Prof. Nurullah ARSLAN
Director

June 2015

SYNTHESIS AND CHARACTERIZATION OF SINGLE-ION CONDUCTING POLYMER ELECTROLYTES FOR LITHIUM-ION BATTERIES

Aneeka Zaheen Kamal

M.S. Thesis – Chemistry
June 2015

Thesis Supervisor: Assoc. Prof. Dr. Sevim ÜNÜGÜR ÇELİK

ABSTRACT

Single-ion conducting polymer electrolytes have become crucial in lithium-ion batteries due to the elimination of the polarizing effects. In this study, lithium oxalate polyacrylic acid borate and lithium oxalate polyvinyl alcohol borate complexes were produced and then blended with poly (polyethylene glycol methacrylate) (PPEGMA). In addition poly (2-acrylamido-2-methyl-1-propanesulfonic acid-co-polyethylene glycol methacrylate) copolymer was synthesized with free radical polymerization and then Li ion was exchanged with hydrogen in the sulfonic acid group. The resulting single-ion conducting polymer electrolytes were characterized via Fourier transform infrared spectroscopy (FTIR). The thermal properties were analyzed with thermogravimetric analysis (TGA) and differential scanning calorimetry (DSC). The effect of PPEGMA on the ionic conductivity was investigated with impedance analyzer and the maximum ionic conductivity was measured as 2.89×10^{-4} S/cm at 100 ºC for LiPVAOB-60PPEGMA.

Keywords: Polyvinyl alcohol, polyacrylic acid, poly (2-acrylamido-2-methyl-1-propanesulfonic acid), polyethylene glycol methacrylate, ionic conductivity, Li-ion battery

LITYUM IYON PILLER IÇIN TEK IYON ILETKEN POLIMER ELEKTROLIT SENTEZI VE KARAKTERIZASYONU

Aneeka Zaheen Kamal

Yüksek Lisans Tezi –Kimya
Haziran 2015

Thesis Supervisor: Assoc. Prof. Dr. Sevim ÜNÜGÜR ÇELİK

ÖZ

Tek iyon iletken polimer elektrolitler, lityum-iyon pillerde polarize etkileri ortadan kaldırdığı için çok önemli hale gelmiştir. Bu çalışmada lityum okzalat poliakrilik asit borat ve lityum okzalat polivinil alkol borat kompleksleri üretildi ve poli (polietilenglikol metakrilat) (PPEGMA) ile kompozit yapıldı. Ayrıca serbest radikal polimerizasyon ile poli (2-akrilamido-2-metil-1-propansülfonik asit-ko-polietilen glikol metakrilat) kopolimeri sentezlendi ve Li iyonu ile sülfonik asit grubundaki hidrojen yer değiştirildi. Üretilen tek-iyon iletken polimer elektrolitler Fourier transform infrared spektroskopisi (FTIR) ile karakterize edildi. Termal özellikler termogravimetrik analiz (TGA) ve diferansiyel taramalı kalorimetre (DSC) ile analiz edildi. PPEGMA içeriğinin iyonik iletkenliğe etkisi impedans analizör ile araştırıldı ve en yüksek ilektenlik LiPVAOB-60PPEGMA için 100 $^{\circ}$C'de 2.89×10^{-4} S/cm olarak ölçüldü.

Anahtar Kelimeler: Polivinil alkol, poliakrilik asit, poli (2-akrilamido-2-metil-1-propansülfonik asit), poli (etilen glikol) metakrilat, iyonik iletkenlik, Li-iyon pil

To my lovely parents, Naz Hussain & Khalid Kamal, my awesome sister Esha Mahee Kamal and Mr. Ahmet Andac.

ACKNOWLEDGEMENT

This goes without mention from the bottom of my heart, that it is Almighty Allah who has blessed me in every step of the way in making me finish my thesis at the right time, despite all the hurdles, without whom none of this would have been possible.

These acknowledgements are to extend my sincere thanks and gratitude to those who have provided assistance, support, insight, and knowledge in order to make this research possible. Without their help, I could not have completed this work.

I would like to thank my supervisor Assoc. Prof. Sevim ÜNÜGÜR ÇELİK. She has provided wonderful guidance and support through the entire research process, and her encouragement made the project enjoyable and successful. Her calming personality and open-door policy was always appreciated. My utmost respect and sincere gratitude goes to her for giving me the opportunity to work with her and giving me the confidence to pursue my research.

This thesis would not have been possible without my family's love and encouragement. I would specially like to thank my Mother who has been my biggest strength and support system in my academic life, helping me in ways I will forever be indebted to.

I would like to thank my lab colleagues Abdulmalik Yusuf, Hamide Aydin, Murat Ercan, Mehmet Kaynak & Mehmet Ş. Tutgun from the very bottom of my heart for helping in every way possible. My utmost gratitude goes out to Abbakar Hamisu & Umar Yushau for boosting up my confidence and encouraging me in every step. Lastly, I would like to take this chance to thank all my dear friends for always being there for me.

TABLE OF CONTENTS

LIST OF TABLE

TABLE

LIST OF FIGURES

FIGURES

LIST OF SYMBOLS AND ABBREVIATIONS

SYMBOL/ABBREVIATION

AIBN	Azobisisobutyronitrile
AMPS	2-Acrylamido-2-methyl-1-propanesulfonicacid
DMF	N-N-Dimethylformamide
LIB	Lithium ion battery
LIB's	Lithium ion batteries
LiOPAAB	Lithium oxalate polyacrylic acid borate
LiPVAOB	Lithium polyvinyl alcohol oxalate borate
PAA	Polyacrylic acid
PAABA	Polyacrylic acid-boric acid
PAMPS	Poly (2-acrylamido-2-methyl-1-propanesulfonicacid)
PE	Polymer electrolyte
PE's	Polymer electrolytes
PEGMA	Polyethylene glycol methacrylate
PEO	Poly (ethylene) oxide
PPEGMA	Poly (polyethylene glycol methacrylate)
PVA	Polyvinyl alcohol
PVABA	Polyvinyl alcohol-boric acid
SPE	Solid polymer electrolyte
SPE's	Solid polymer electrolytes

CHAPTER 1

INTRODUCTION

Energy is a necessity for the modern society, a drug facilitating the needs of every 21st century human in order to sustain a normal living. In order to meet the growing demand of energy, extensive research and development have been conducted. After years of hard work scientists currently have been able to crack the code in producing clean and secure energy as well as energy storage and efficient energy resources.

Electronic devices such as portable cell phones and laptops incorporate the use of polymer electrolytes, especially 'lithium-ion batteries (LIB's), which are currently the 'in thing' in the scientific community as storage devise. LIB's are quite in demand in the energy industry due to their inherent low safety risks, the ability to be formed into thin films, light weight and flexibility [1]. Compared to conventional and electrochemical systems based on hydrocarbons LIB's have zero carbon emission during operation, another massive advantage [43]. Other than portable devises LIB's are an optimal power source for hybrid electric vehicles (HEVs), plug in hybrid electric vehicles (PHEVs) and electric vehicles [63].

Like any other battery, the building block of a typical LIB consists of a transition-metal oxide cathode ($LiCoO_2$, $LiMnO_2$ etc.), carbon anode (graphite, graphene etc.), a separator and an electrolyte. Electrolyte is one of the key components of rechargeable LIB, it facilitates the ion transport between electrodes in the device [58]. It is essential to develop an electrolyte with high ionic conductivity along with thermal and electric stability.

The use of single-ion conduction is fairly a new concept that is been used in LIB's. Widespread commercial use of single ion systems in energy devices will require

more sophisticated polymer electrolyte formulations and a better understanding of the nature of charge storage.

The general goal of this work is to synthesize and investigate properties of novel solid single-ion conducting polymer electrolytes (PE's) with ethylene oxide (EO) units for use in LIB. Here three separate polymer electrolyte (PE) synthesis are reported, initially polyethylene glycol methacrylate) (PEGMA) was polymerized to obtain poly (polyethylene glycol methacrylate) (PPEGMA), which was later blended with the PE's.

In the 1st study a novel single-ion conducting electrolyte, lithium polyvinyl alcohol oxalate borate (LiPVAOB), based on polyvinyl alcohol, boric acid, lithium carbonate and oxalic acid was synthesized. The obtained PE was then blended with different ratios of poly (polyethylene glycol methacrylate) (PPEGMA).

In the 2nd study polyacrylic acid, boric acid, lithium carbonate and oxalic acid were used to synthesize lithium oxalate polyacrylic acid borate (LiOPAAB). The resulting PE was then blended with different ratios of PPEGMA.

In the 3rd and final study 2-Acrylamido-2-methyl-1-propanesulfonicacid (AMPS) was copolymerized with several ratios of polyethylene glycol methacrylate (PEGMA) to obtain poly(2-acrylamido-2-methyl-1-propanesulfonicacid-co-poly(ethyleneglycol) methacrylate) copolymer. To the resulting copolymer lithium hydroxide was added for the purpose of ion exchange to obtain a single-ion conducting PE.

The PE's were characterized via FT-IR, TGA, and DSC. The morphology of the PE's were investigated using SEM. The Li-ion conductivity was measured using dielectric-impedance analyzer and the electrochemical properties are investigated with the help of Cyclic Voltammetry.

CHAPTER 2

LITHIUM-ION BATTERIES

2.1 INTRODUCTION

Batteries are electrochemical devices that store chemical energy and convert it into electrical energy to power numerous devices [2, 3].The basic building blocks of a typical battery consist of one or more cells, and each cell is made up of a positive electrode, a negative electrode, separator and an electrolyte (Figure 2.1).

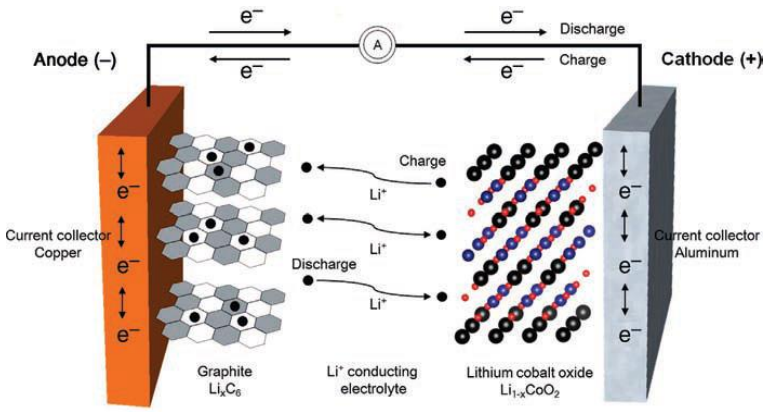

Figure 2.1 Representation of a Battery [2]

Batteries can be categorized into two important classes: primary and secondary batteries. The chemical reactions that occur are not reversible in a primary battery making them non-rechargeable, secondary batteries are the opposite. The chemical reactions are reversible making it possible for them to be recharged. Such batteries can

be charged and discharged several times whereas primary batteries are used once and disposed[4,5]

2.2 CHEMISTRY IN BATTERY

The key process of generating energy is by the substitution of atoms and ions by the withdrawal or supplying electrons from the external circuit, in other words electrochemical reactions taking place at the two electrodes (anode and cathode). Each electrode undergoes electrochemical reaction known as half-cell reaction.

When a battery is being discharged electrons flow form the anode towards the cathode. The anode is being oxidized and as the cathode accepts electrons it gets reduced. The operation of a battery during discharge is illustrated in Figure 2.2. Discharging is the process to convert the chemical energy carried out by the battery into electrical energy[4, 5].

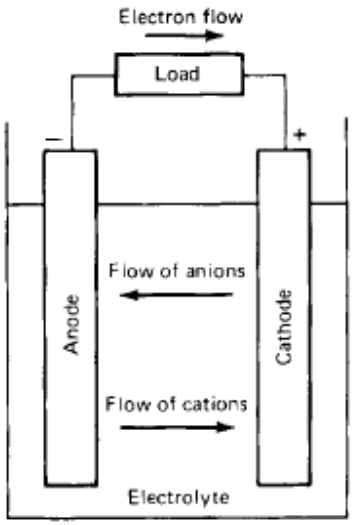

Figure 2.2 Electrochemical operation of a cell during discharge [5]

The electrochemical half-cell reactions occurring during discharge can be written as follows (assuming Zn as the anode and Cl_2 as the cathode):

At negative electrode: oxidation

$Zn \rightarrow Zn^{+2} + 2e^-$

At positive electrode: reduction

$Cl_2 + 2e^- \rightarrow 2Cl^-$

Overall reaction (discharge):

$Zn + Cl_2 \rightarrow Zn^{+2} + 2Cl^- (ZnCl_2)$

The charging of a battery is the exact opposite of discharging. The electron flow is in the opposite direction, oxidation occurs at the positive electrode and reduction at the negative (Figure 2.3). Oxidation and reduction both simultaneously occur at the same electrode in a secondary battery, meaning the cathode during discharge can be anode during charging and vice versa [4, 5].

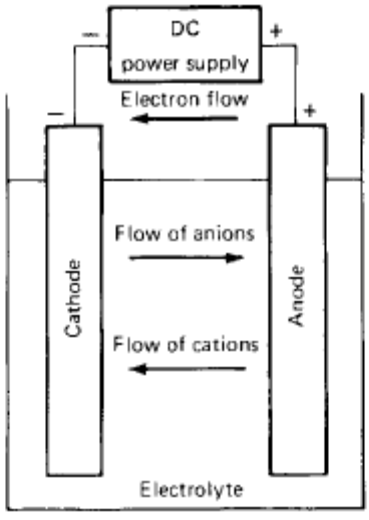

Figure 2.3 Electrochemical operation of a cell during charging [5]

The electrochemical half-cell reactions occurring during charging can be written as follows:

Negative electrode: reduction

$Zn^{+2} + 2e^{-} \rightarrow Zn$

Positive electrode: oxidation

$2Cl^{-} \rightarrow Cl_2 + 2e^{-}$

Overall reaction (charge):

$Zn^{+2} + 2Cl^{-} \rightarrow Zn + Cl_2$

The separator and the electrolyte, each has its unique role in the function of the battery. The separator for instance plays a crucial role in the whole system, to keep the electrodes from coming in contact with each other at all times, and hence preventing short-circuits. The electrolyte acts as a carrier medium, ferrying the ions between the electrodes, where the chemical reactions occur to generate the electricity [4, 5].

2.3 TYPES OF BATTERIES

Secondary batteries are being used worldwide in a wide range of applications, from automotive applications to portable devices. Currently they have gained a good reputation as a power source for electric and hybrid electric vehicles. Examples of secondary batteries include lead-lead dioxide (lead-acid), nickel-cadmium, nickel-metal hydride and lithium-ion.

2.3.1 Lead-acid

Lead-acid batteries came to form with the research conducted by Raymond Gaston Plante in 1860, the oldest known secondary battery. Lead-acid batteries are manufactured in a range of size and design with energy densities ranging from 10-44 Wh Kg^{-1} and 50-111 Wh dm^{-3}. Generally lead-acid batteries are used as power storage

in vehicles; however they can be used in portable devises as well. A typical lead-acid battery is constructed with lead oxide as the positive electrode, metallic lead as the negative electrode and sulfuric acid (37% by weight or 1.28 specific gravity) as the electrolyte. Both the electrode are converted to lead sulfate during discharging, the process just reverses during the charging [4, 5]. The electrochemical half-cell reactions occurring during discharge and charging can be written as follows:

Negative electrode:

$Pb \rightarrow Pb^{2+} + 2e^{-}$

Positive electrode:

$PbO_2 + 4H^{+} + 2e^{-} \rightarrow Pb^{2+} + 2H_2O$

Overall reaction:

$Pb + PbO_2 + 2\ H_2SO4 \rightarrow 2\ PbSO_4 + 2H_2O$

2.3.2 Nickel- cadmium

In the late 19th century Waldemar Jungner developed the nickel-cadmium battery. Nickel- cadmium batteries are mainly used as power supplies for stationary, traction and aircraft engine with energy densities form 18-75 Wh kg^{-1} and 30-220 Wh dm^{-3}. NiCd battery is constructed with cadmium hydroxide as the negative electrode with up to 25% iron and minute amount of Ni and graphite whereas the positive electrode is made up of nickel oxide with cobalt oxide, and electrolytes with aqueous solutions of 20-30% potassium hydroxide with up to 2% lithium hydroxide [4, 5].The electrochemical half-cell reactions occurring during discharge and charging can be written as follows:

Negative electrode:

$Cd + 2OH^{-} \rightarrow Cd(OH)_2 + 2e^{-}$

Positive electrode:

$Ni(O)OH + H_2O + e^{-} \rightarrow Ni(OH)_2 + OH^{-}$

Overall reaction:

$$Cd + 2Ni(O)OH + 2H_2O \rightarrow Cd(OH)_2 + 2Ni(OH)_2$$

2.3.3 Nickel-Metal Hydride

The construction of Nickel-Metal Hydride (NiMH) is somewhat similar to Nickel-Cadmium battery. The positive electrode and the electrolyte is the same, the only thing different is the negative electrode, a metal alloy combined with polytetrafluoroethylene (PTFE). NiMH batteries are not as much powerful as NiCd batteries and less tolerant to overloading. However they have greater energy densities ranging from 23-92 Wh kg^{-1} and 32-332 Wh dm^{-3} [4, 5]. The electrochemical half-cell reactions occurring during discharge and charging can be written as follows:

Negative electrode:

$$MH + OH^- \rightarrow M + H_2O + e^-$$

Positive electrode:

$$Ni(O)OH + H_2O + e^- \rightarrow Ni(OH)_2 + OH^-$$

Overall reaction:

$$MH + Ni(O)OH \rightarrow M + Ni(OH)_2$$

2.3.4 Lithium-ion

The history of the development of the lithium-ion battery (LIB) is the quest for the development of a high voltage battery, the higher the voltage the higher the energy. The historical figure to invent the very first battery was Alessandro Volta (1745-1827) over 200 years ago, Professor of Physics at the University of Pavia Italy. This invention of his became the technological sensation of the time, soon battery sales started for the production of railway signals and telegraph [4, 5].

In the year 1859 the first secondary battery (lead-acid) was demonstrated by French chemist Gaston Plante. Later in the mid-1970s (precisely 1976) M. S.

Whittingham demonstrated a new form of secondary battery, the very first LIB. Eventually in 1990 Sony produced the first LIB composed of graphite anode, lithium cobalt oxide cathode and an organic carbonate-based solution with lithium salt as the electrolyte and has been producing ever since with some modification in the construction. Since then, LIB's have dominated the power storage industries for electronic and portable devises and is preferred over lead-acid and NiMH batteries. As illustrated in Figure 2.4 the specific energy of a secondary LIB is 5 times more than that of lead-acid batteries and 3 times as much as a NiMH battery [2, 4].

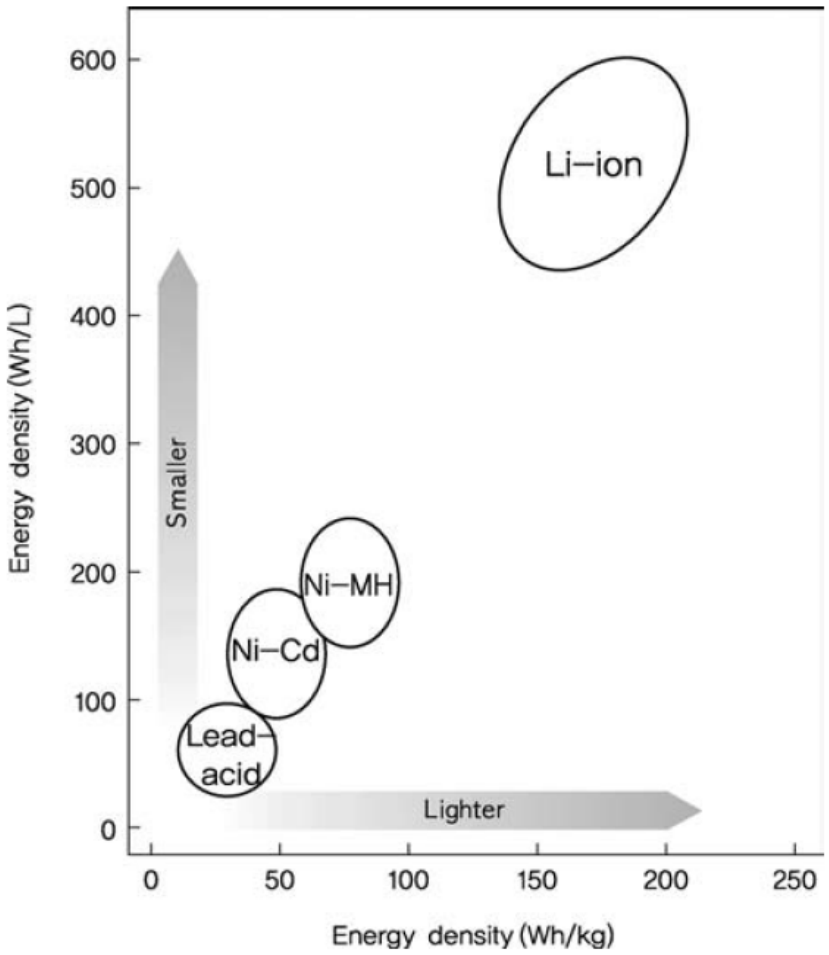

Figure 2.4 Energy density changes with evolution of batteries [2]

Lithium Ion batteries can be categorized according to cell shapes and component material. The diverse shapes that it can acquire include the typical cylindrical laptop batteries, prismatic cells for mobile devices, coin shaped batteries and pouch shaped cells in aluminum plastic composites, as illustrated in Figure 2.5.

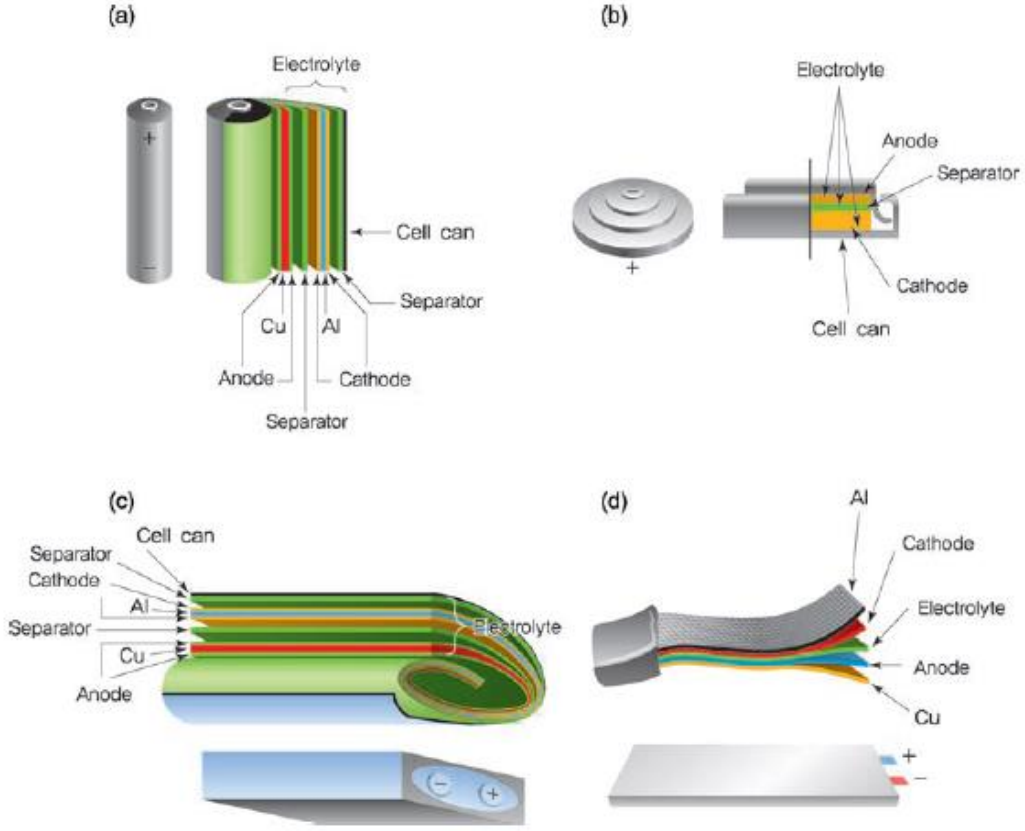

Figure 2.5 Diverse shapes acquired by LIB's: (a) cylindrical, (b) coin, (c) prismatic [2]

The building block of a typical LIB consists of a transition-metal oxide cathode, carbon anode, a separator and polymer based electrolyte. LIB's function by charging and discharging chemical mechanism. During charging mechanism the lithium ions are intercalated into the molecular structure of the electrodes (Equation 2.1). Reduction occurs during the charging mechanism, as the lithium ions are intercalated in between the graphite layers.

Charge (2.1)

$$C_6 + x\,Li^+ + x\,e^- \rightleftharpoons Li_xC_6$$

Discharge

Discharging is the exact opposite of charging mechanism, where the lithium ions deintercalate from the anode (graphite) (Figure 2.6). The whole cycle of charging and discharging mechanism repeats several times in the battery [2, 5, 6].

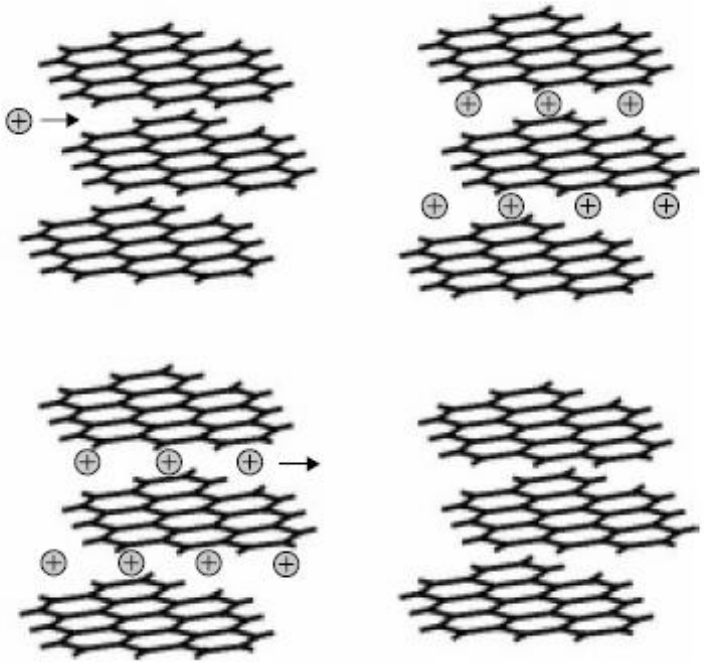

Figure 2.6 Lithium ion (Li^+) intercalation into and deintercalation out of graphite during lithium ion battery charging and discharging. The circles represent lithium ions (Li^+) [6]

Intercalation and deintercalating of the lithium ion occurs at the same electrode during the entire cycle of charging and discharging. This phenomenon of oxidation and

reduction both occurring at the same electrode is termed “rocking chair” or “shuttlecock” mechanism (Figure 2.7).

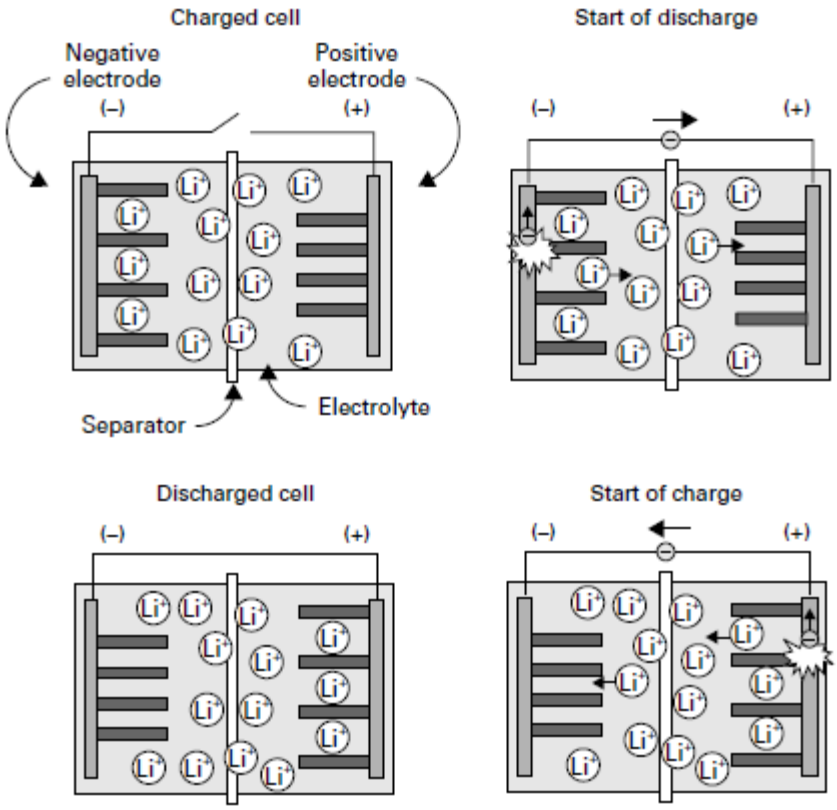

Figure 2.7 Discharge and charge processes [6]

Several studies have been conducted on oxides of lithium and a transition metal as the cathode, lithium-cobalt oxide ($LiCoO_2$), lithium-manganese oxide ($LiMnO_2$), lithium-iron phosphate($LiFePO_4$) are some of the common materials used as cathodes. Commercial LIB utilizes lithium cobalt oxide ($LiCoO_2$) as the cathode, with conductivity of 10^{-3} S/cm^{-1} [5-8].

In terms of symmetry, $LiCoO_2$ are in the *r3m* space group, where the transition metal and lithium ion occupy octahedral 3(a) and 3(b) sites and the oxygen ions at 6(c) sites respectively. Resulting in a layered giant structure, with alternating cations and anions, and with oxygen ion in a cubic shape. Whereas $LiMnO_2$ acquire spine structure,

with *Fd3m* symmetry in which the transition-metal, lithium ion and oxygen ions occupy octahedral 8(a), tetrahedral 16(c) and 32(c) sites respectively [5, 8].

A variety of carboneous materials can serve as the anode in a LIB, carbon nanotubes, distorted carbons and graphite the major types of carbon anodes [7]. The typical carbon anode currently in use for anode material is graphite. Graphite has layers of carbon atoms to form a hexagonal structure, much like a bee hive as illustrated in Figure 2.8. Weak Van der Waals forces hold the structure together in to an ABAB stacking sequence. Artificial graphite can be synthesized from pyrolyzed carbon at a very high temperature, around 3000 °C [4-6].

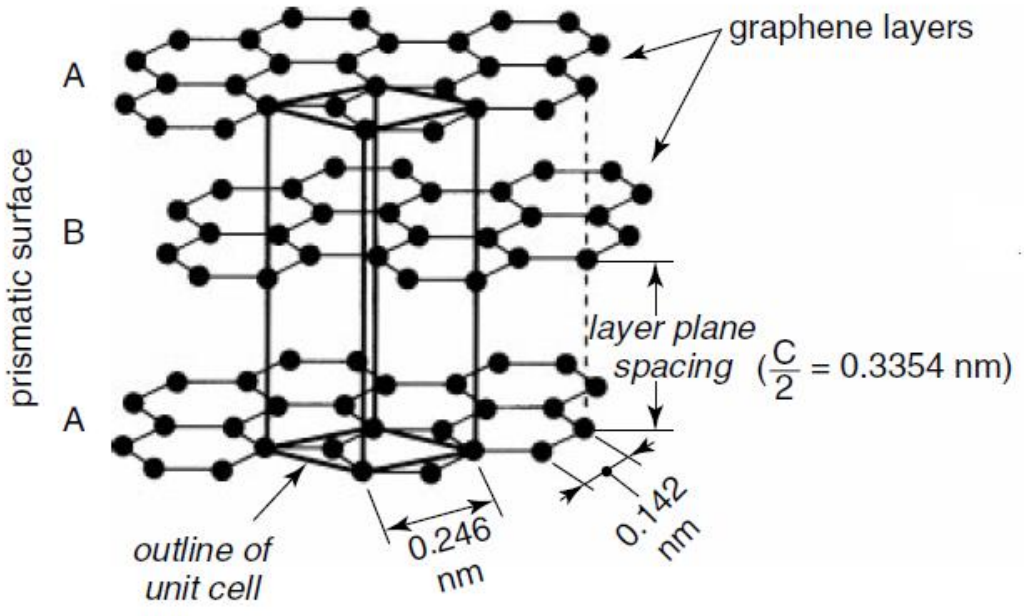

Figure 2.8 Crystal structure of hexagonal Graphite [7]

The choice of electrolyte plays a key role in the function of the LIB. Currently three major types of electrolytes are available depending on the physical state, solid, liquid and gel electrolyte [9, 10]. The ideal choice of an electrolyte for a typical LIB is either solid or gel electrolyte over liquid electrolyte. Keeping safety in mind it is best to

choose solid or gel electrolyte, since liquid electrolytes can be very hazardous due to the organic solvents being used, such as lithium hexafluorophosphate ($LiPF_6$) or lithium bis(perfluoroethanesulfonyl)imide ($LiN(SO_2C_2F_5)_2$ better known as LiBETI. The solvents are flammable by nature and may leak causing fire, which may lead to an explosion as well [11].

The separator which one might think is not as important as the electrodes and the electrolyte, but in fact it has a very important role in keeping the battery intact and functioning properly. It acts as barrier between the anode and cathode so they don't come in contact with each other causing short-circuit. Organic polymers such as polypropylene (PP), polyethylene (PE) etc. are some examples that are being used in the construction of separator. Current separators in use might have attractive mechanical strength and electrochemical stability, but when it comes to melting temperature and glass transition (T_g) they have a poor reputation. Numerous researches are being conducted at the moment in order to overcome these weaknesses and to produce a novel separator [12-14].

2.4 POLYMERIC ELECTROLYTES

2.4.1 Introduction

Peter Wright and Michel Armand, the pioneers of the polymer electrolytes (PE's) introduced a new class of solid ionic conductors in 1970s since Michael Faraday confirmed the existence of ionic conductivity in solid state [15-17]. Solid polymer electrolytes(SPE's) have had the spot light ever since, due to the wide range of application in electrochemical devises such as LIB, super capacitors, fuel cell, solar cell, actuators, portable devises e.g. cell phone, laptops etc. [18-25]. A desirable Polymer electrolyte(PE) must possess: (a) High conductivity at ambient and sub ambient temperature [26], (b) good mechanical strength, (c) both thermal and electrochemical stability and (d) compatible with electrode in order to be applicable in such diverse application [27-29].

In order to circumvent the possible issues faced by conventional liquid electrolyte, a promising approach is utilizing SPE's in constructing LIB's. SPE's tend to be safer due to their flame resistance nature [30, 31]. Other desirable properties making them a promising approach to circumvent the issues faced by liquid electrolytes are: (a) flexibility, (b) lack of toxicity, (c) design and shape flexibility, (d) light weight, (e) ease in process ability [25, 32-36] and (f) dual function as a separator and ionic conductor [11, 36].

2.4.2 Structural features of Solid Polymer Electrolytes

Normally SPE's are formulated by dissolving a salt species (alkali salt) in a solid polymer host [33, 35, 37]. The complex formed by the polymer and salt supplies mobile ions, the polymer host has a critical part in the ionic transport process of the PE. Ion transport arises in amorphous phase aided by the segmental motion of the polymer chain [38]. In such kind of electrolyte, conductivity is believed to rise from the ion migration through intra-inter-chain hopping mechanism between the coordinating sites continuously triggered by local segmental motion of the polymer chain [15]. Hence, a promising polymer host must meet certain criteria: (a) donor atom or groups capable of forming coordinating bond with cation, (b) minimal bond rotation barriers for simple bond rotation of polymer chain and (c) a significant distance from the coordinating centers for numerous intra-inter polymer bonding with cations [15, 39]. Several polymer host such as such as poly(ethylene oxide) (PEO) [40], polymethyl methacrylate (PMMA) , Chitosan (CS) [41], polyacrylonitrile (PAN) [42] and polyvinyl chloride (PVC) [43] fit the criteria's, however PEO still remains the main interest of research as a suitable polymer host due to its ability to solvate a numerous range of alkali cation [35, 44-46]. PEO in its pure state lacks in conductivity, at room temperature has maximum conductivity of 10^{-9} S/cm [38]. Incorporating salts species (LiX) into the polymer can enhance conductivity and reach between 10^{-8} - 10^{-4} S/cm [47].

Early researchers claimed that the helical polymer chain of PEO were important for ion transport. However, this incorrect idea got proven wrong with NMR experiments on $LiCF_3SO_3$. Experiments conducted by the author showed that the ion transport occurs in indeed in the amorphous region just about the glass transition temperature T_g and the hopping rate of cation is limited due to the comparative slow segmental motion of the

polymer chains, hence the low conductivity. Figure 2.9 illustrates the ion transport in PEO based PE's. Another way to describe the low conductivity is by addressing the low dielectric constant of PEO. Equation 2.2 gives the conductivity of the PE, where σ is the conductivity, *n* the concentration of charge carriers, *q* charge and μ mobility.

$$\sigma = n\, q\, \mu \tag{2.1}$$

From the equation it is seen that the conductivity (σ) is reciprocal to the concentration of charge carriers (*n)*. The low value of dielectric constant causes intense ion-ion interaction which leads to ion pair formation and elevated ion aggression. The charge carrier concentration (*n*) drops due to the formation of ion pairs and so does the conductivity **(**σ**)** [16].

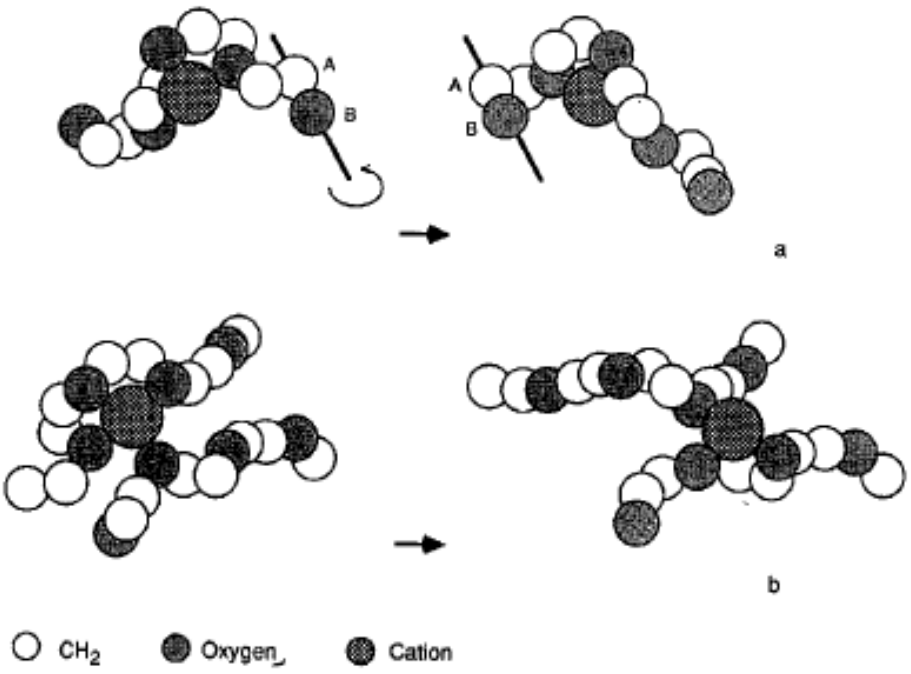

Figure 2.9 Representation of ion migration in PEO-based PE's [15]

2.5 SINGLE-ION CONDUCTORS

Conventional SPE's currently used in LIB's make use of dual conducting system, with PEO based host polymer, where salt solvation occurs due to Lewis acid–base interaction of ether oxygen atom with the cation. The ion conduction in such kind of electrolytes arises as the cation moves through the amorphous phase. Unlike the cation, the anions tend to have weaker interactions with polymer chain which allows them to move easily [30, 48-51].

Numerous research have shown the cations tend to have a very low fraction of the conductivity (transference number), ranging from 0.3-0.5, implying majority arising from the anion [11, 18, 28, 52]. Mobility of both the ions lead to electrode polarization, reducing the overall battery performance as a result of high internal resistance, loss of voltage and unwanted reactions such as dendritic growth causing an early battery failure. Further degradation occurs in the cation conductivity due to the mobility of both the ions [28, 48-50].

In order to cope up with the polarization complications arising from dual ion conducting system, a new approach of single-ion conductors was recently contrived. A single-ion conducting electrolyte is constructed from a polymeric/copolymeric lithium salt. The anions are immobilized by covalently bonding them to the polymeric/copolymeric backbone, permitting only lithium ion transport during discharging and charging [35, 53]. The transference number of single-ion conductors are close to unity since the anions become a part of the polymer chain [36] which reduces the salt concentration gradient hence low electrode polarization [54]. Until now several type of single ion conductors have been reported, such as comb-like polymer [55-58], composite polymer [59-64], network polymers [63, 64] and linear polymer [64, 65].

L. M. Bronstein and group have described a composite PE consisting of poly(ethylene glycol) and an organic-inorganic component. The resulting PE had a 0.9 Li^+ transference number and exhibited highest conductivity at room temperature, which was 1×10^{-4} S/cm [32].Shaowei Fang and group proposed a single-ion conducting copolymer composed of lithium (4-styrenesulfonyl)(trifluoromethanesulfonyl)imide

(LiSTFSI) and methoxy-polyethylene glycol acrylate (MPEGA). They reported a Li^+ transference number of 0.9 and found that the conductivities of the Li[PSTFSI-co-MPEGA] are 1-3 folds higher than the blended counter parts. The maximum ionic conductivity achieved was 7.6×10^{-6} S/cm at 25 ºC and 10^{-4} S/cm at 60 ºC. Figure 2.10 schematically shows the synthesis of the single-ion conducting copolymer [30].

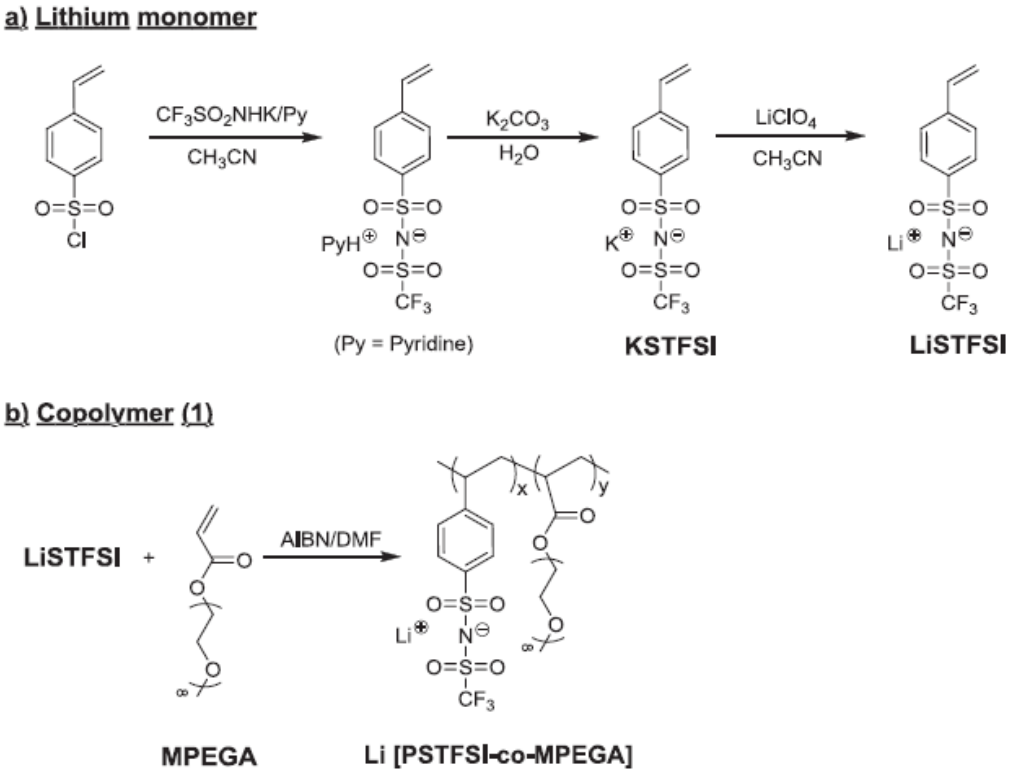

Figure 2.10 Single-ion conducting copolymer [30]

Rachid. M and group proposed a single-ion conducting copolymer composed of $-SO_2\ N^--\ SO_2-\ CF_3$ anionic groups associated with a lithium cation and attached to a polystyrene chain. The resulting PE, poly(4 styrenesulfonyl)(trifluoromethanesulfonyl)imide (PSTFSI) exhibited ten times higher conductivity (10^{-5} S/cm) compared to lithium poly(styrene sulfonate) [11].

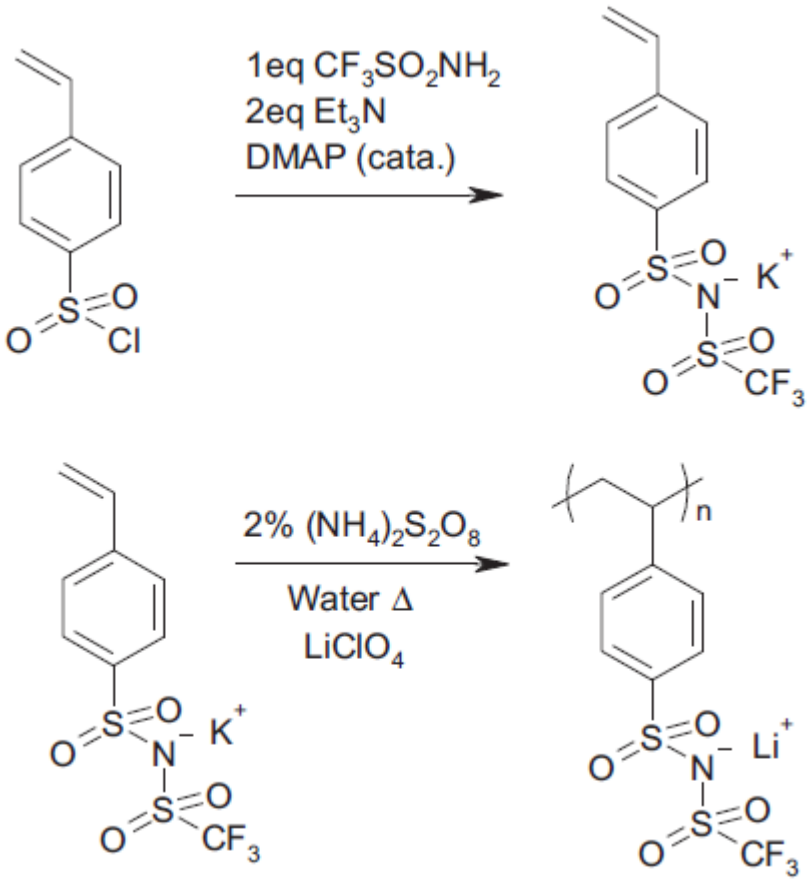

Figure 2.11 Synthesis of STFSIK monomer and of PSTFSI [11]

Single-ion conducting PE's generally tend to have poor conductivities at ambient and medium temperature, with in the range of $1 \times 10^{-8} – 1 \times 10^{-7}$ S/cm [30].However if ion diffusivity is enhanced by allowing selected organic solvents to flow into the polymer matrix with appropriate pores to facilitate ion diffusion as suggested by Rupesh et al., the ionic conductivity can be elevated as close to 1×10^{-3} S/cm at ambient temperature. Rupesh Rohan, et al., studies proved not only do they have high ionic conductivities, but also they seem to be both thermally and electrochemically more superior to conventional liquid electrolytes, a perfect and safe choice for a wide range of battery devices [53].

CHAPTER 3

EXPERIMENTAL PROCEDURES

3.1 MATERIALS AND METHODS

PEGMA (M_n = 360g/mol) (Figure 3.1), lithium hydroxide (>98%), oxalic acid (>99%), DMF (>99%) and lithium carbonate (>99%) were purchased from Sigma Aldrich Chemicals. Toluene (>99.9%), AIBN, PVA (degree of hydrolization ≥98% M_w = 72,000) (Figure 3.2) and AMPS (>99%) were purchased from Merck. Acrylic acid (>99%) and boric acid (>99%) were purchased from Alfa Aesar.

3.1.1 Synthesis of poly (polyethylene glycol methacrylate) (PPEGMA)

The initial step is to successfully synthesize PPEGMA form the monomer PEGMA using AIBN initiator at 70 ºC in toluene according to Figure 3.1.

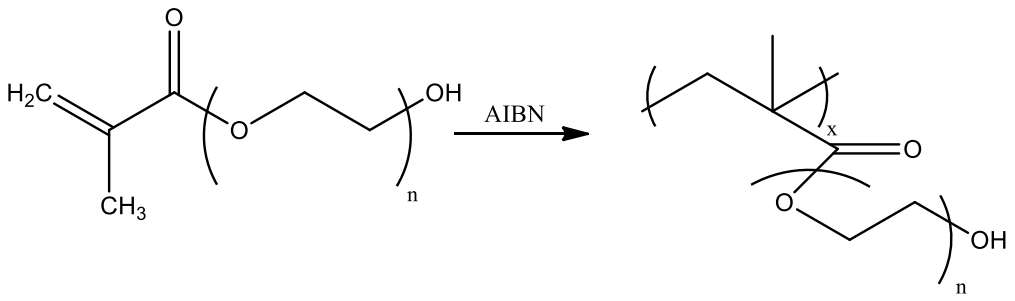

PEGMA **PPEGMA**

Figure 3.1 Synthesis of poly (polyethylene glycol methacrylate) (PPEGMA)

3.1.2 Synthesis of polyvinyl alcohol (PVA) - poly (polyethylene glycol methacrylate) (PPEGMA) based composite electrolytes

The PE was prepared by the reaction of PVA, lithium carbonate, boric acid and oxalic acid in accordance to Figure 3.2. A homogeneous and transparent solution was obtained after Boric acid and PVA were dissolved into distil water and heated to 80 ºC for 5 h. Then oxalic acid and lithium carbonate were added and refluxed for 24h at 100 ºC. Before proceeding further the solution (LiPVAOB) was cooled to room temperature.

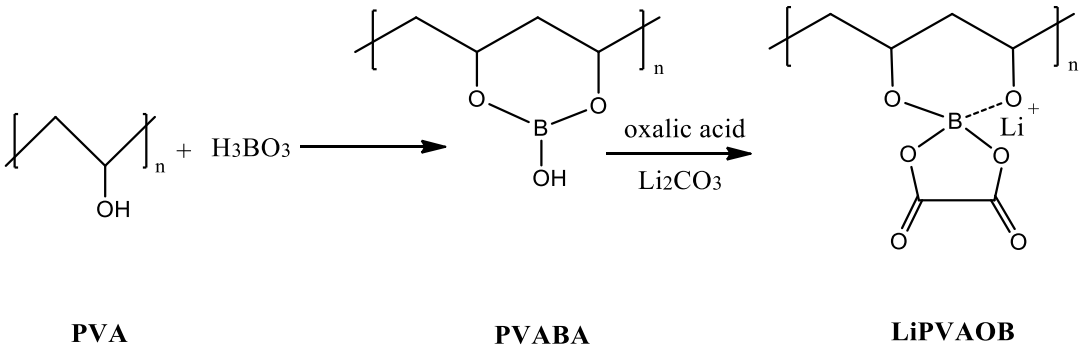

PVA **PVABA** **LiPVAOB**

Figure 3.2 The preparation process of LiPVAOB

After cooling, the solution was divided equally into six parts. Then each part was blended with different molar ratios of PPEGMA (0 %, 10%, 20%, 40%, 60% & 80%). Known amount of LiPVAOB and PPEGMA were added to labeled vials inside the fume cupboard and were stirred continuously for 2 h at room temperature. The blends were then cast on labeled Teflon petri dishes and left overnight to dry at room temperature. The blends were further dried in vacuum oven at 70 ºC for 48 h.

3.1.3 Synthesis of polyacrylic acid (PAA) - poly (polyethylene glycol methacrylate) (PPEGMA) based composite electrolytes

Initially acrylic acid was polymerized using AIBN initiator at 60 ºC in toluene. Afterwards the PE was prepared by the reaction of PAA, lithium carbonate, boric acid and oxalic acid in accordance to Figure 3.3. A homogeneous and transparent solution was obtained after Boric acid and PAA were dissolved into distil water and heated to 80 ºC for 5 h. Then oxalic acid and lithium carbonate were added and refluxed for 24h at 100 ºC. The solution was cooled to room temperature before proceeding any further.

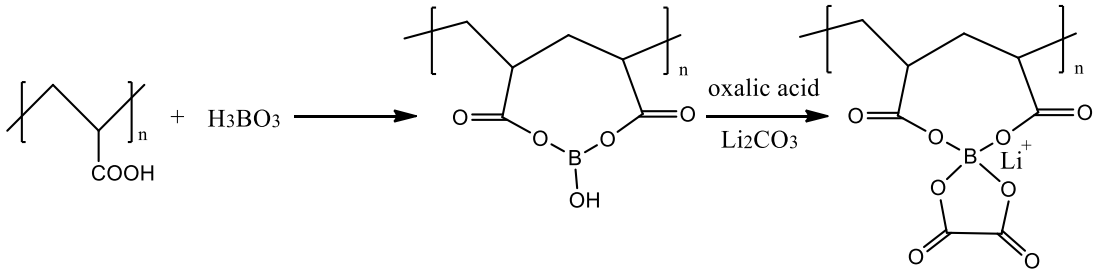

Figure 3.3 The preparation process of LiOPAAB

After cooling, the solution was divided equally into six parts. Then each part was blended with different molar ratios of PPEGMA (0 %, 10%, 20%, 40%, 60% & 80%). Known amount of LiOPAAB and PPEGMA were added to labeled vials inside the fume cupboard and were stirred continuously for 2 h at room temperature. The blends were later cast on labeled Teflon petri dishes and were left overnight to dry at room temperature. The blends were further dried in vacuum oven at 70 ºC for 48 h.

3.1.4 Synthesis of poly (acrylamido-2-methyl-1-prapanesulfonicacid-co-poly (ethylene glycol) methacrylate) copolymer electrolyte

The copolymer was prepared by radical polymerization of PEGMA and AMPS monomers according to Figure 3.4. Three different samples of copolymers were prepared according to mole ratio (1:1/2, 1:1, & 1:2). The polymerization was carried out in DMF and AIBN to initiate the reaction. Reactants were stirred continuously for 5 h at

60 ºC to obtain light yellow copolymer which were then cooled at room temperature. After cooling, the copolymers were vacuum filtrated with ether to remove any trace of monomers, later cast on labeled Teflon Petri dishes and left over night to dry in room temperature. The copolymer was further dried in a vacuum oven at 60 ºC for 48 h.

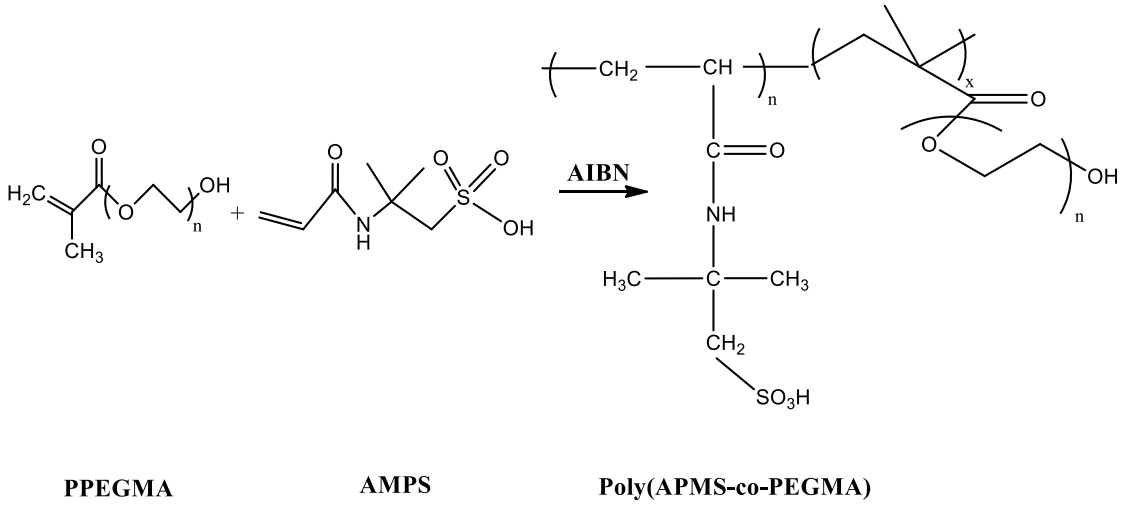

Figure 3.4 Synthesis of Poly(AMPS-co-PEGMA)

Ion exchange was carried out on the copolymer with LiOH (0.1M) solution. In three labeled vials different copolymers samples were added along with known volume of LiOH solution. The resulting mixture was stirred for 24 h at room temperature, later vacuum filtrated with distil water and finally cast on labeled Teflon petri dishes to dry overnight in room temperature . The copolymers were further dried in a vacuum oven at 60 ºC for 48 h.

3.2 CHARACTERIZATION

3.2.1 FT-IR Spectroscopy

Fourier-Transform Infrared Spectroscopy (FT-IR) is one of the important and well-known analytical techniques, for the identification of compounds and structural determination. Virtually any state of sample can be examined with this technique.

Liquids, solids, powder, fibres, polymers, drugs, paints, coatings etc. all can be examined. This spectroscopy technique is based on the idea of the interference of radiation between two beams to yield an interferogram or most commonly known as spectrum. A typical FT-IR curve is plotted with transmittance over wavelength range.

FT-IT spectra of pure sample and composites were scanned using Bruker Alpha-P in ATR system between 4000-400 cm^{-1}.

3.2.2 Thermogravimetric Analysis (TGA)

Thermogravimetric Analysis is form of thermal technique which measures weight loss of a sample as it is either heated or cooled in a controlled environment. TGA is used for the determination of thermal stability, and decomposition temperature. It can also be used to determine the composition and for identification of polymers by comparing thermal decompositions patterns. TGA is an essential technique used in many industrial applications such as food, pharmaceutical and petrochemical application. The outcome of the TG curves can be influenced by elements like the mass, volume and physical form of sample, the shape and type of the crucible, the environment pressure and rate of scan. Typical TG curves are plotted with weight loss % in the x-axis against temperature in the y-axis.

Thermal stabilities of pure samples and composites were examined with PerkinElmer Pyris 1 TG Analyzer. Samples were heated in room temperature till 750 ºC under N_2 environment scanning at a rate of 10 ºC/min.

3.2.3 Differential Scanning Calorimetric (DSC) Analysis

DSC is a thermal analysis technique in which a samples heat flow is measured as a function of time and temperature. A sample of known mass is heated and cooled over a rage of temperature and the resulting heat flow is measured. DCS technique is used to detect transitions such as melting point(T_m), glass transition (T_g), crystallization (T_c) and heat capacity. The glass transition is a very important parameter in order to understand polymer transition. A typical DSC curve is plotted with heat flow on the x-axis and with temperature on the y-axis.

DSC measurements of pure sample and composites were carried out with PerkinElmer Pyris 1 DSC instrument under N_2 environment, with a scanning rate of 10 ^oC/min.

3.2.4 Scanning electron microscopy (SEM)

Scanning electron microscope is a form of electron microscope; images of sample are produced by scanning it by a focused beam of electrons. The samples morphology and composition can be determined by SEM technique. Normally raster scan pattern is used for scanning the electron beam. An image is produced by combing the signal that is detected and the position of the beam. The resolution of an image produced by SEM is more than one nanometer.

The morphologies of samples were observed with scanning electron microscopy (SEM, Philips XL30S-FEG). Prior the SEM measurement all the samples were sputtered with gold.

3.2.5 Impedance Spectroscopy

Impedance Spectroscopy is a technique that measures the dielectric (conductivity) properties of a substance as a function of frequency. It is an essential standard characterization technique used in various applications such as corrosion, plating, batteries, fuel cells, etc.

Novocontrol dielectric-impedance analyzer was used to measure the alternating current (AC) conductivities of the polymer and copolymer samples in the frequency range from 0.1 Hz to 3 MHz as a function of temperature. Sample pellet (with a diameter of 10 mm and a thickness of approximately 0.5mm) were sandwiched in between two gold-coated electrodes.

3.2.6 Cyclic Voltammetry (CV)

CV is a form of potentio dynamic electrochemical measurement. In a typical cyclic voltammetry experiment the working electrode potential is drawn linearly against time. These cycles of ramps in potential may be repeated as many times as desired. A typical cyclic voltammogram is plotted with working electrode potential current on y-

axis and applied voltage on the x-axis. It is an essential technique for the investigation of electrochemical properties of an analyte in a solution.

CV of LiOPAAB-60PPEGMA polymer electrolyte was obtained with potentiostat Metrohm Autolab (Multichannel-M101 Model). A ten-electrode test cell was constructed utilizing stainless steel as the working electrode and Li as the counter and reference electrode. All the scans were made between 0 and 5V at a scan rate of 10 mV/s.

CHAPTER 4

RESULT AND DISCUSSION

4.1 FT-IR

4.1.1 FT-IR of PVA-PPEGMA based composites

FT-IR Spectra of PVA, PPEGMA, PVABA and LiPVAOB membrane are shown Figure 4.1. Pure PVA shows characteristic absorptions at 3278, 2890, 1143 and 1090 cm^{-1}, corresponding to *v* O-H, *v* C-H, *v* C-C-O and *v* C-O, respectively [49]. After reaction of PVA with Boric acid (PVABA) the peak at 3278 and 2890 cm^{-1}, corresponding to *v* O-H and *v* C-H became broader and an additional new peak at 650 is observed which is attributed to the formation of B-O bond. One major factor affecting the IR absorption is the degree of hydrogen bonding. Hydrogen bonding tends to alter the electron cloud, which then alters the resonant frequency of a particular bond. Different molecules tend to have slightly different hydrogen bonding states, which leads them to have slightly different absorption frequencies and thus the broad band. Apart from these C-O exhibit peak at 1095 cm^{-1} [49, 66]. In PPEGMA *v* C=O exhibits a strong peak at 1720 cm^{-1} and the two bands seen at 1311 and 1246 $cm^{-1}$are due to C-O stretching of the ester group. Apart from these *v* O-H and *v* C-H exhibit peaks at 3474 and 2870 cm^{-1}, respectively.

After the addition of lithium carbonate and oxalic acid to PVABA, the complex LiPVAOB forms. LiPVAOB exhibits new additional peaks at 1333 and 1670 cm^{-1}, corresponding to the anti-symmetric stretching vibration of the B-O bond and *v* C=O [49, 67]. The peak seen at 3297 cm^{-1} is attributed to *v* O-H, which is caused by the absorption of water by LiPVAOB in air due to the presence of strongly polarized Li^{+}

ions [49]. The successful formation of the LiPVAOB is clearly evident from these characteristic absorption bands.

Figure 4.2 represents the spectra of LiPVAOB-XPPEGMA blended with different percentage of PPEGMA. As the level of the PPEGMA in the sample increases it is noticed that the O-H band broadens and C-H band starts to appear which as well becomes intense as the amount of PPEGMA in sample increases.

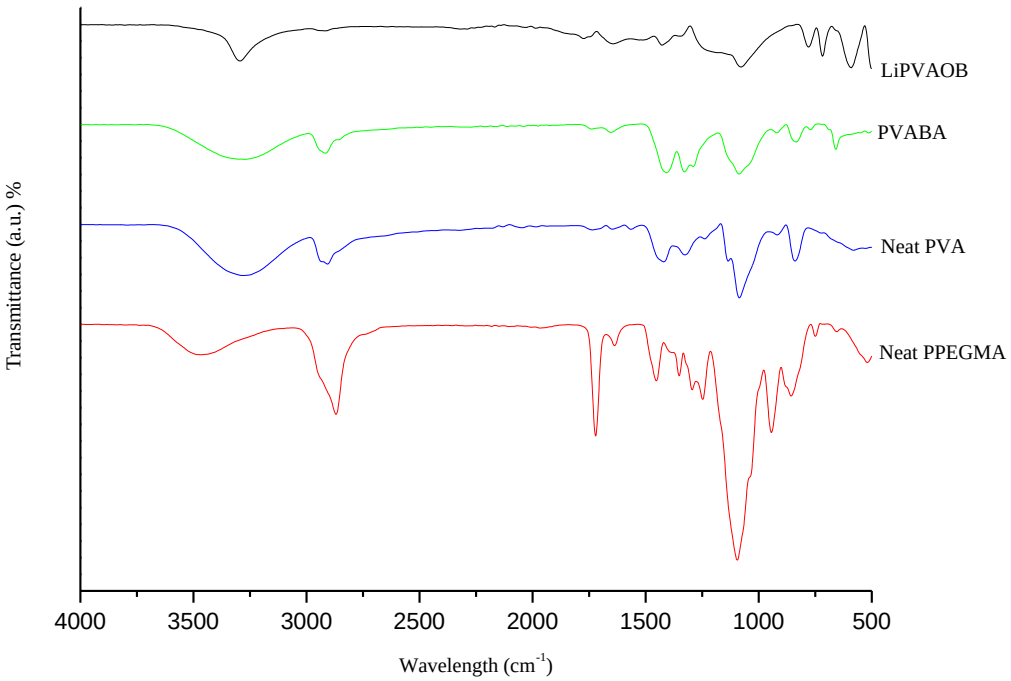

Figure 4.1 FT-IR spectra of PVA, PPEGMA, PVABA & LiPVAOB

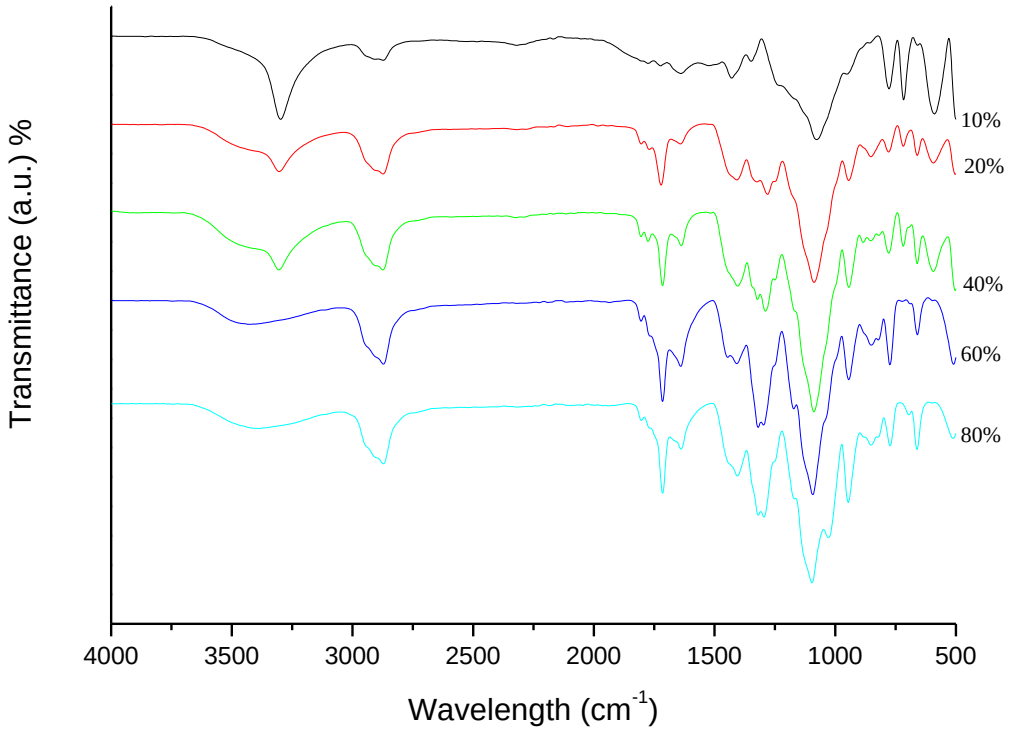

Figure 4.2 FT-IR spectra of LiPVAOB-XPPEGMA X=10, 20, 40, 60 & 80

4.1.2 FT-IR of PAA-PPEGMA Composites

FT-IR Spectra of PAA, PPEGMA, PAABA and LiOPAAB membrane are shown Fig. 4.3. PAA shows characteristic absorptions at 3306, 2932, 1655 and 1300 cm^{-1}, corresponding to *v* O-H, *v* C-H, *v* C=O and *v* C-O , respectively [48]. After reaction of PAA with boric acid additional three new peaks are observed at 664, 800 and 1554 cm^{-1}, corresponding to B-O vibration, *v* C-O-B-O-C and B-O-C vibration respectively. The peak at 1625 cm^{-1}, and two peaks at 1388 and1302 cm^{-1} may be due to C=O and C-O respectively. In PPEGMA C=O gives a strong peak at 1720 cm^{-1} and the two bands seen at 1311 and 1246 cm^{-1} are due to C-O stretching of the ester group. Apart from these O-H and C-H exhibit peaks at 3474 and 2870 cm^{-1} respectively.

The FT-IR spectrum of LiOPAAB exhibits additional two new peaks, 1321 cm^{-1} which is attributed to the anti-symmetric stretching vibration of the B-O bond and 1180 cm^{-1} due to C-O-C anti-symmetric stretching. Quite similar to PVA-PPEGMA

electrolytes, the peak seen at 3207 cm^{-1} is attributed to *v* O-H, which is caused by the absorption of water by LiOPAAB in air due to the presence of strongly polarized Li^{+} ions [48, 49].

Figure 4.4 represents the spectra of LiOPAAB-XPPEGMA blended with different percentage of PPEGMA. Just like the previous section, increment in PPEGMA concentration broadens the O-H band, also C-H band appears and becomes intense.

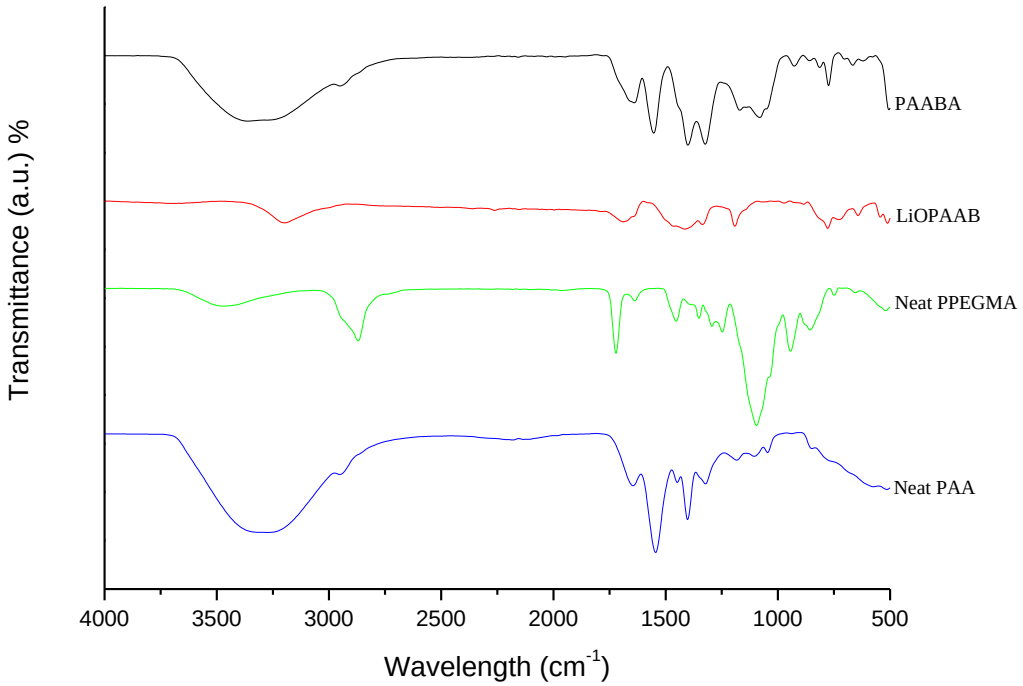

Figure 4.3 FT-IR spectra of PAA, PPEGMA, PAABA & LiOPAAB

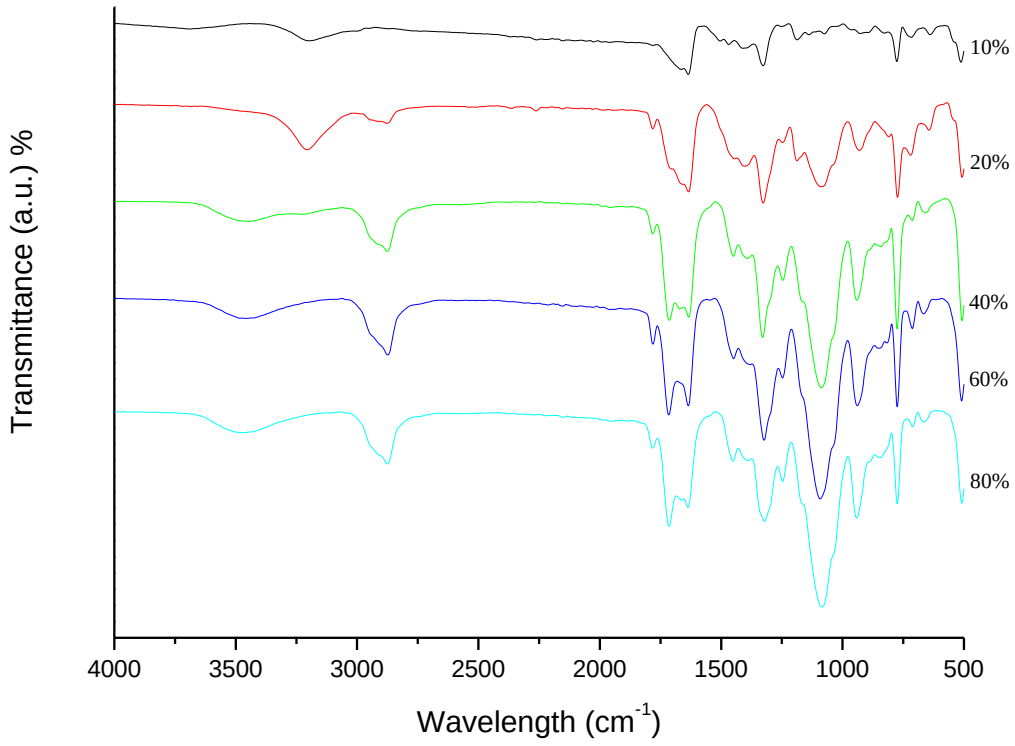

Figure 4.4 FT-IR spectra of LiOPAAB-XPPEGMA X=10, 20, 40, 60 & 80

4.1.3 FT-IR of PAMPS-PPEGMA Copolymer

FT-IR spectra of Pure PAMPS, PPEGMA and Poly (AMPS-co-PEGMA) with different ratios of PEGMA are shown in Figure 4.5. Pure PAMPS shows characteristic absorptions at 1015, 1234, 3303, 1412, 1317 and 1082 cm^{-1}, corresponding to O=S=O, SO3H, N-H, O=C-N (amide I), O=C-N (amide II) and *v* C-N respectively [68, 69].

The copolymers exhibited absorptions at 1723 cm^{-1} (C=O), 1655 cm^{-1} O=C-N (amide I), 1546 cm^{-1}O=C-N (amide II), 1300 & 1280 cm^{-1} (C-O), 1108 cm^{-1} (C-N) and 1035 cm^{-1} (O=S=O) respectively. These absorption bands verify the successful formation of poly (AMPS-co-PEGMA).As X varies from 0.5 to 2 these peaks become more intense [68].

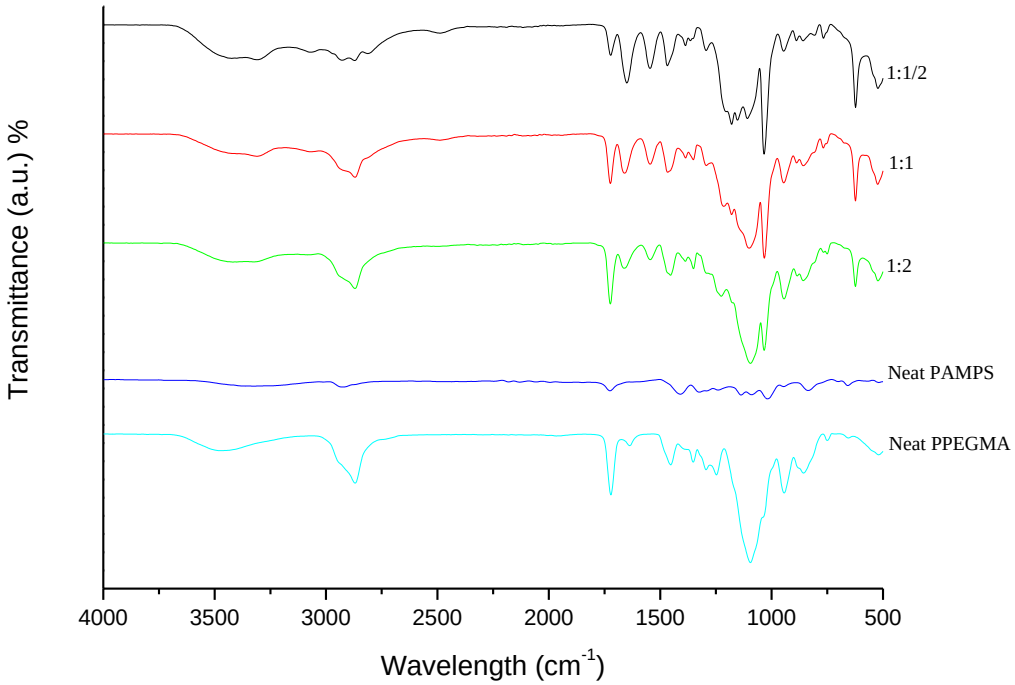

Figure 4.5 FT-IR spectra of PAMPS, PPEGMA & poly (AMPS-co-PEGMA) (1:X) X=0.5, 1 & 2

4.2 THERMO GRAVIMETRIC ANALYSIS (TGA)

4.2.1 TGA of PVA-PEGMA Composites

An important property for polymer electrolytes (PE's) during application of LIB is thermal stability. TGA provides a vague idea about the possible physical changes that may occur during a thermal excitation in a PE when it is applied to working systems [67]. Thermal stability of neat polymers and the electrolytes with different blending ration of PPEGMA were evaluated by TGA.

Figure 4.6 represents the TG thermogram of neat PVA, PPEGMA, PVABA and LiPVAOB. It is reported in the literature that PVA is stable between 215-225 ºC, [49, 66], as seen the PVA being used has a degradation temperature of approximately 223 ºC. The slight weight change between 0-100 ºC may have been due to absorbed humidity or the solvent may not have evaporated properly during the drying steps. The weight loss seen above 200 ºC is due to the decomposition of the polymer chain.

Neat PPEGMA is stable up to 200 ºC. The initial weight loss between 0-100 ºC is due to absorbed humidity or the solvent used may not have been removed. The final weight loss seen at 200 ºC is due to the decomposition of the polymer chain.

As seen PVABA is stable up to 221 ºC, while LiPVAOB has three step decomposition as seen in the graph. The initial weight loss between 0-100 ºC is due to the loss of oxalate complex [70]. The second weight loss is seen at 180 ºC and The final weight loss seen is probably due to the decomposition of the polymer chain around 400 ºC.

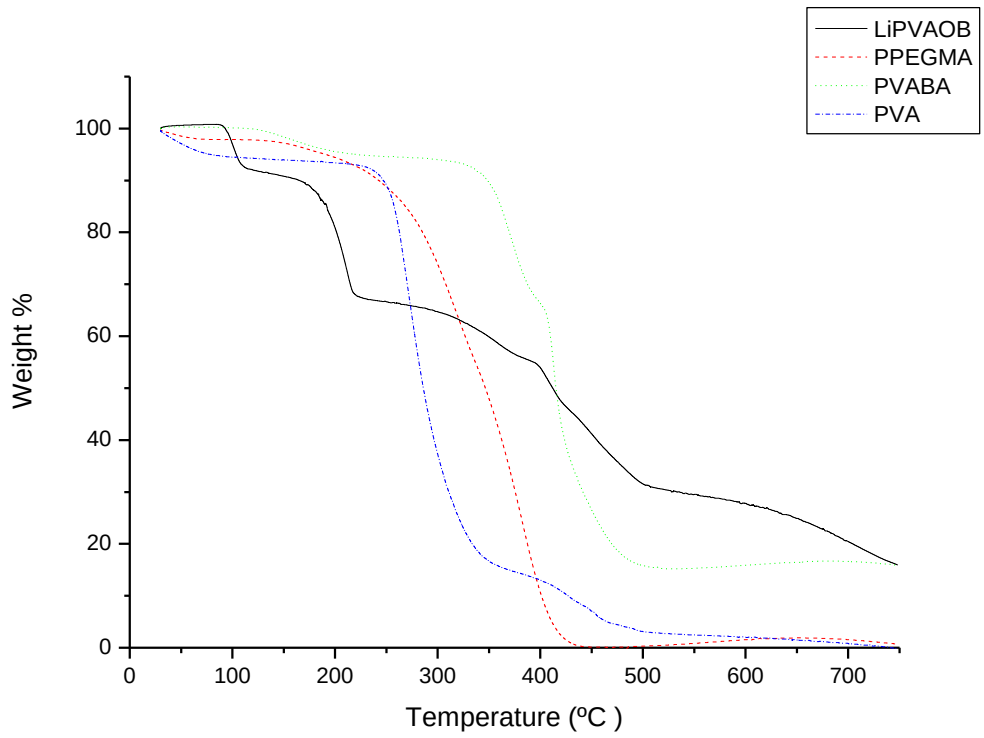

Figure 4.6 TGA curves of PVA, PPEGMA, PVABA and LiPVAOB

The thermal stability was investigated for LiPVAOB after blending with several ratios of PPEGMA. Figure 4.7 represents the thermograms of the polymer electrolytes LiPVAOB-XPPEGMA. From the graphs it is quite obvious all the samples have a three-step weight loss. The initial weight change approximately at 100 ºC may have

been due to decomposition of oxalate complex [70]. The second weight loss observed between 200-300 ºC. The final weight loss around 400 ºC is due to the decomposition of the polymer chain. It is observed that the thermal stability of polymer electrolytes increase as the amount of PPEGMA increases.

Generally LIB's are stable up to 85 ºC then again with the aid of fire-retardants and other additives [48, 49]. PE's containing PPEGMA have excellent thermal stability, much higher than conventional PE's making them a desirable choice of electrolyte in developing of LIB's.

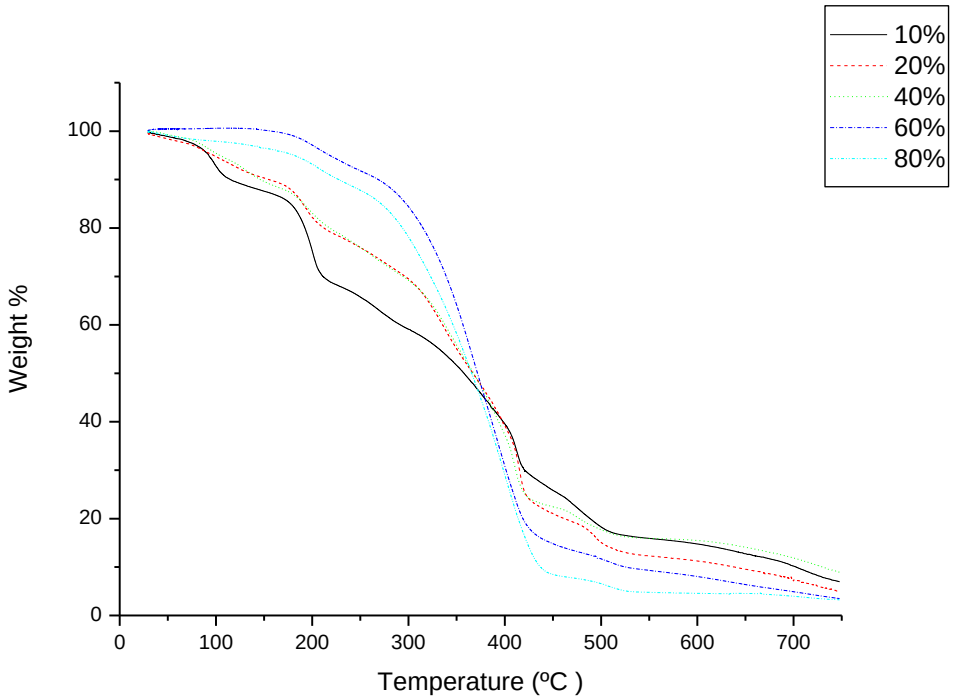

Figure 4.7 TGA curves of LiPVAOB-XPPEGMA X=10, 20, 40, 60 & 80

4.2.2 TGA of PAA-PEGMA Composites

Figure 4.8 represents the TG thermograms of neat PAA, PPEGMA, PAAOB and LiOPAAB. It is reported in literature that PAA is stable thermally up to 210 ºC [48]. The minor weight loss seen below 100 ºC is due to the absorbed humidity or the solvent

may not have evaporated properly during the drying steps. The major weight loss is observed around 200 ºC which is due to the degradation of the material.

The thermal stability of PPEGMA is approximately 200 ºC, whereas for PAABA and LiOPAAB 73 ºC and 118 ºC respectively.

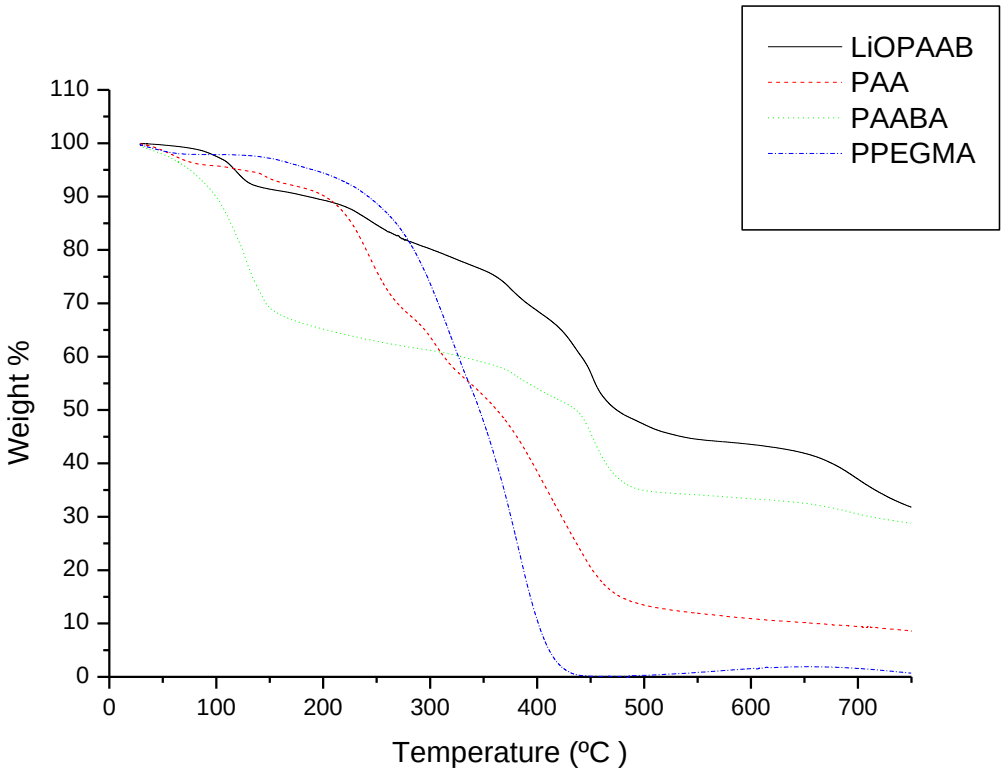

Figure 4.8 TGA curves of PAA, PPEGMA, PAAOB and LiOPAAB

Figure 4.9 represents the thermograms of LiOPAAB-XPPEGMA blends with different percentage of PPEGMA. From the graphs it is quite obvious all the samples initial weight change approximately at 100 ºC may have been due to decomposition of oxalate complex. The second weight loss starts approximately at 200 ºC which is the main decomposition step of the polymer chain. It is observed that the thermal stability of polymer electrolytes increase as the amount of PPEGMA increases. All the samples tend to be stable approximately up to 200 ºC.

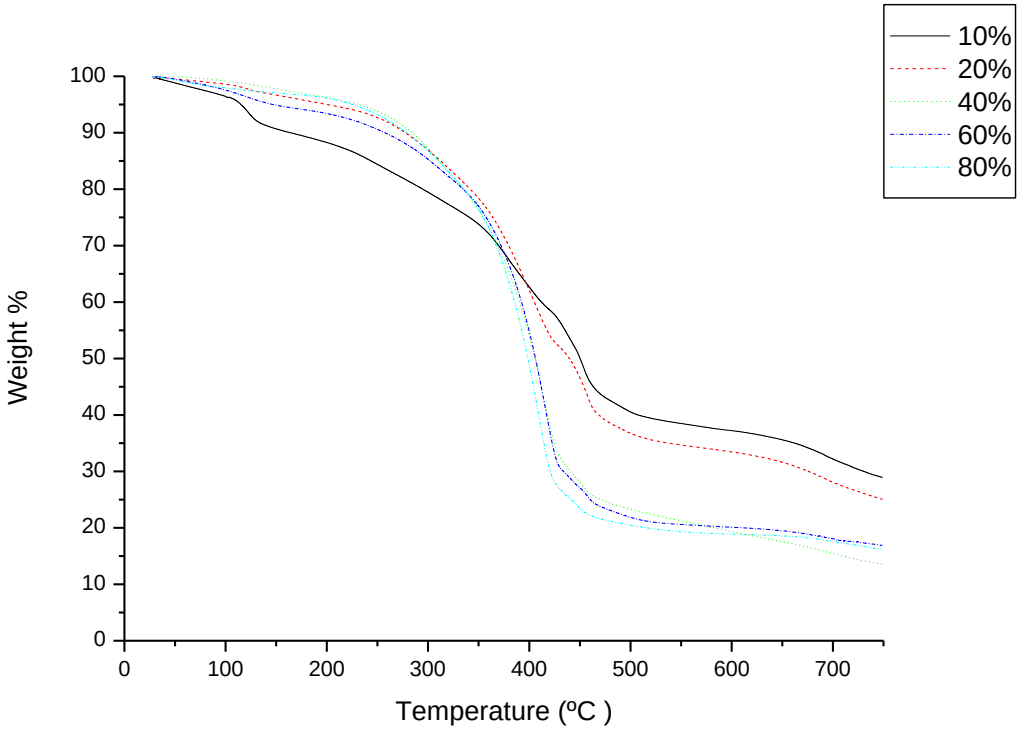

Figure 4.9 TGA curves of LiOPAAB-XPPEGMA X=10, 20, 40, 60 & 80

4.2.3 TGA of PAMPS-PEGMA Copolymer

Figure 4.10 represents the thermogram of neat PAMPS,PPEGMA and poly(AMPS-co-PEGMA) with different ratios of PPEGMA. PAMPS is reported to be stable up to 220 ºC [69, 71]. For the PAMPS used in this work, the major weight loss observed beyond 190 ºC is due to the decomposition of the polymer chains; in other word it is stable thermally up to 190 ºC. The slight weight loss between 0-100 ºC that is noticed can be attributed due to the absorption of moisture.

Neat PPEGMA on the other hand is stable up to 200 ºC. The initial weight loss between 0-100 ºC is due to the absorbed humidity or the solvent used may not have been removed. The final weight loss seen at 200 ºC is due to the decomposition of the polymer chain.

All samples of copolymers have an insignificant weight loss seen between 0 -100 ºC attributed due to the absorbed humidity. A significant amount of weight loss is seen as temperature crosses beyond 200 ºC, which corresponds to the thermal decomposition of the polymer chain. It is very clear that as the percentage of PEGMA increases in the samples, the thermal stability increases.

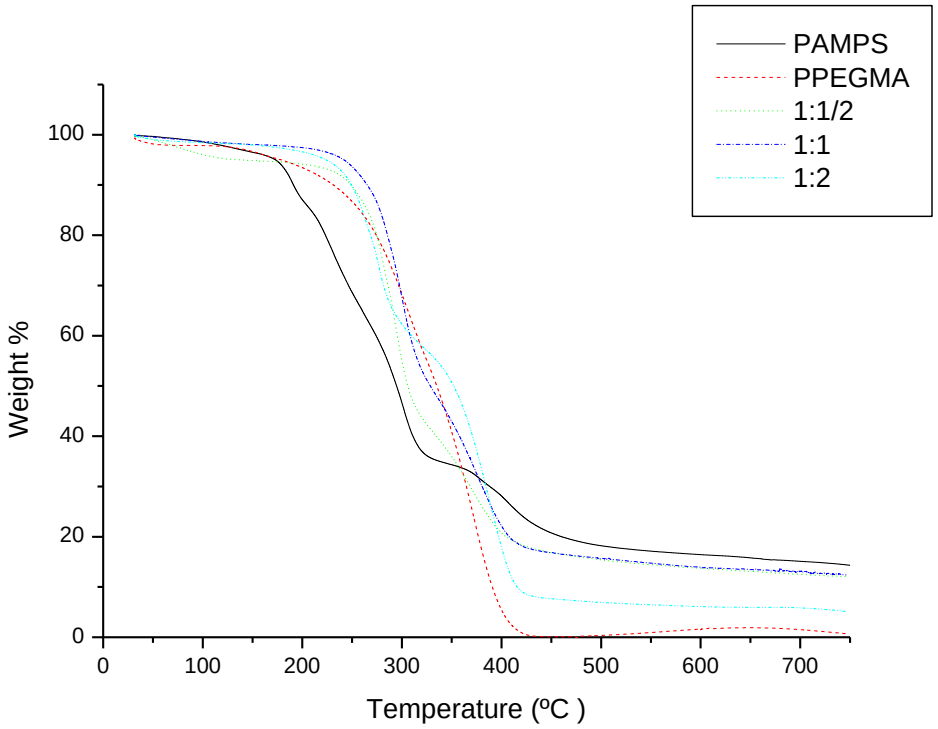

Figure 4.10 TGA curves of poly(AMPS-co-PEGMA) (1:X) X=0.5, 1 & 2 and PAMPS

4.3 DIFFRENTIAL SCANNING CALORIMETTRY (DSC) ANALYSIS

4.3.1 DSC of PVA-PPEGMA composite

Figure 4.11 shows the DSC curves of neat PVA, PPEGMA and LiPVAOB. The second heating curves of all samples were analyzed. Neat PVA did not have a T_g however PVA in literature is reported to have a Tg at 88 ºC [72]. PPEGMA shows a clear and sharp T_c approximately at 142 ºC, whereas LiPVAOB exhibits a broad T_m approximately at 121.34 ºC.

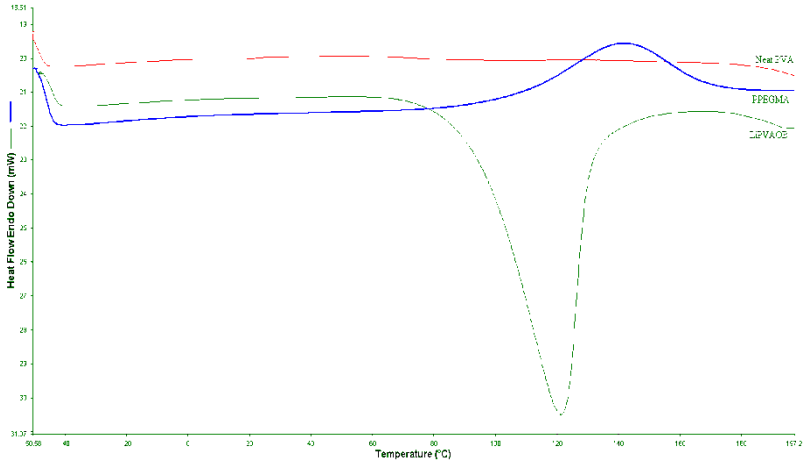

Figure 4.11 DSC curves of Neat PVA, PPEGMA and LiPVAOB

Figure 4.12-4.13 shows the DSC curves of the PE's LiPVAOB-XPPEGMA. The PE's LiPVAOB-XPPEGMA (X= 10, 20 & 40) seem to exhibit a clear ad sharp T_m at 118 ºC, an indication of crystallinity in the PE's. However LiPVAOB-60PPEGMA and LiPVAOB-80PPEGMA exhibit T_c at 147 ºC and 142 ºC respectively. Clearly as the amount of PPEGMA increase the PE's exhibit T_c and starts to lose the crystalline characteristic.

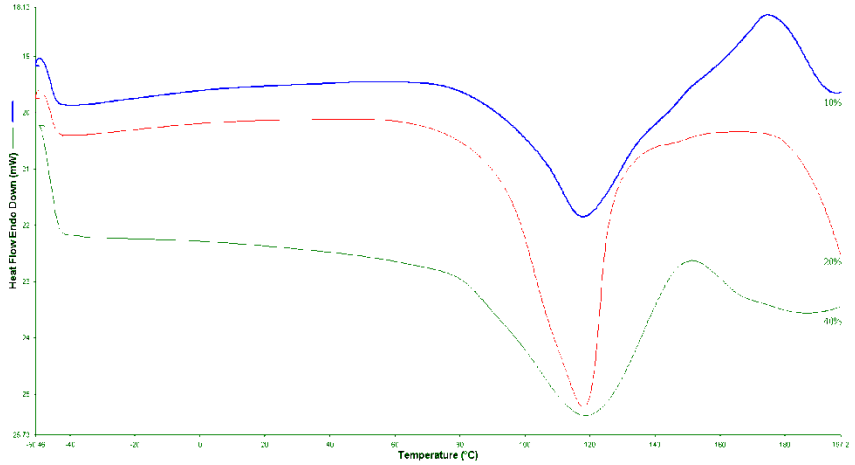

Figure 4.12 DSC curves of LiPVAOB-XPPEGMA X=10, 20 & 40

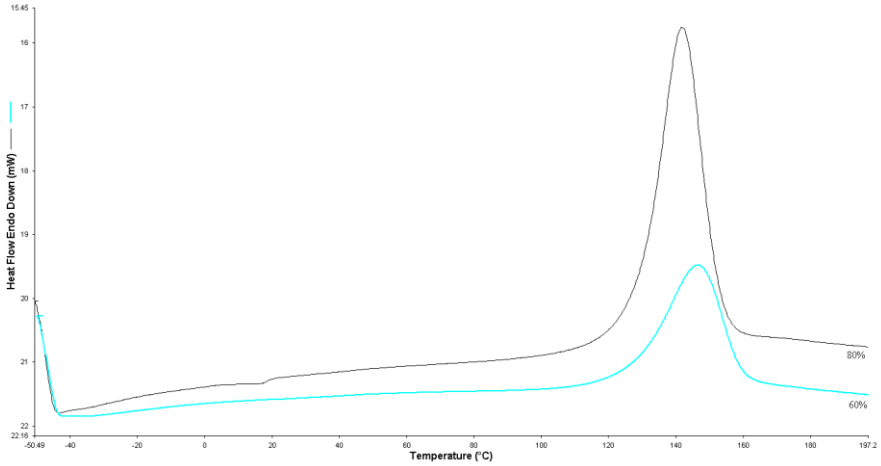

Figure 4.13 DSC curves of of LiPVAOB-XPPEGMA X= 60 & 80

4.3.2 DCS of PAA-PPEGMA composite

Figure 4.14 shows the DSC curves for neat PAA, PPEGMA and LiOPAAB. The reported T_g value in the literature for PAA is 106 ºC [73], for the PAA being used in this work T_g was observed at 90 ºC. LiOPAAB also exhibits a sharp T_m approximately at 124 ºC.

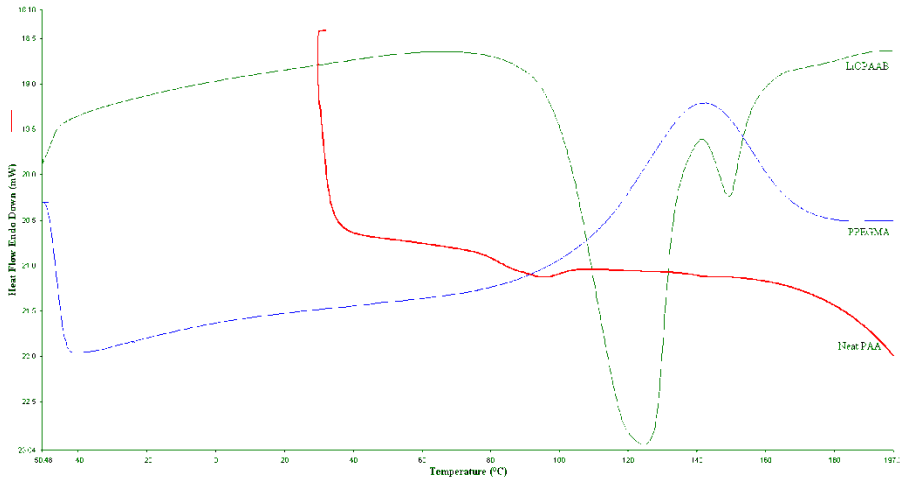

Figure 4.14 DSC curves of Neat PAA, PPEGMA and LiOPAAB

Figure 4.15 shows the DSC curves of the PE's LiOPAAB-XPPEGMA. LiOPAAB-10PPEGMA exhibits a clear and sharp T_m at 133 ºC and the rest LiOPAAB-XPPEGMA (X= 20, 40, 60 & 80) exhibit T_g at 88, 89, 91 and 92 ºC respectively. With the addition of more PPEGMA the PE's tend to exhibit more amorphous character.

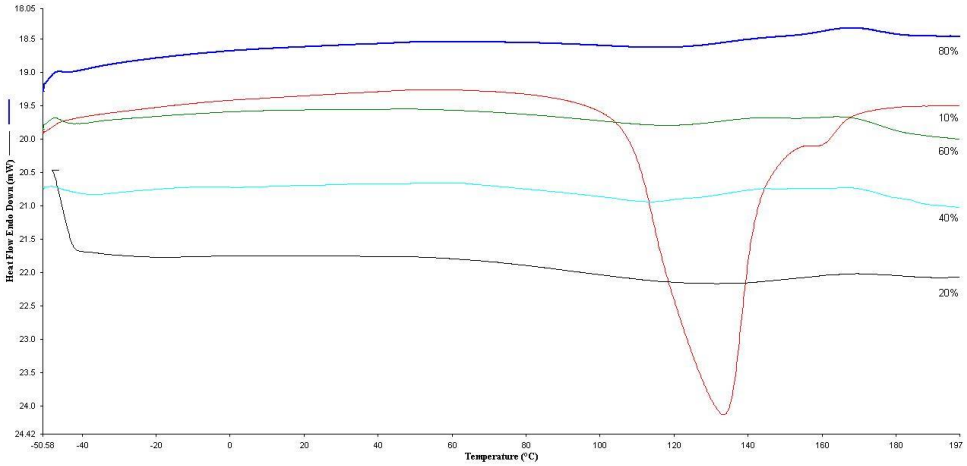

Figure 4.15 DSC curves of LiOPAAB-XPPEGMA X=10, 20, 40, 60 & 80

4.3.3 DSC of PAMPS-PPEGMA copolymer

Figure 4.16 shows the DSC curves for poly (AMPS-co-PEGMA) (1:X) X=0.5, 1 & 2. The reported T_g value in the literature for PAMPS is 108 ºC [69].The PPEGMA used in this work shows a clear and sharp T_c approximately at 142 ºC . poly (AMPS-co-PEGMA) (1:1/2) exhibits a T_g approximately at 102 ºC, poly (AMPS-co-PEGMA) (1:1) exhibits a T_g approximately at 89 ºC however poly (AMPS-co-PEGMA) (1:2) had no visible T_g.

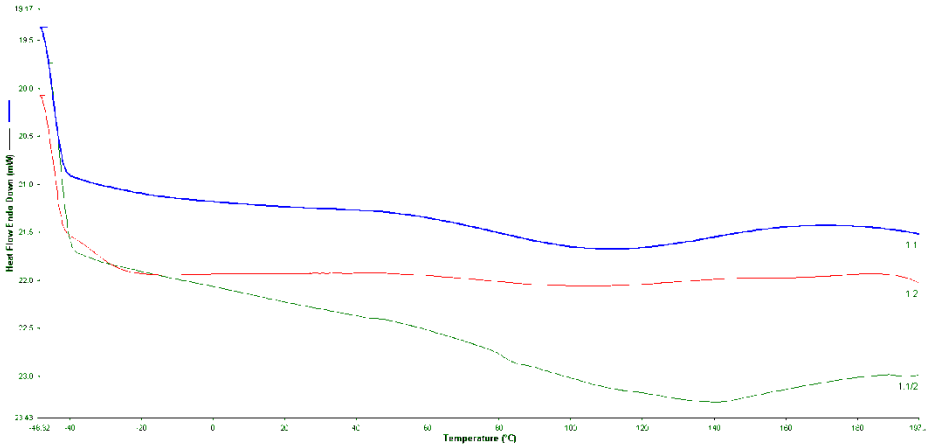

Figure 4.16 DSC curves of poly(AMPS-co-PEGMA) (1:X) X=0.5, 1 & 2 and PAMPS

4.4 SCANNING ELECTRON MICROSCOPY (SEM)

The morphology of LiPVAOB-40PPEGMA, LiOPAAB-20PPEGMA and poly(AMPS-co-PEGMA) (1:1) was examined by SEM and the result are shown in Figure 4.17. For all samples a homogeneous dispersion was observed. No phase separation was observed due to blending; however they appear to be rough and compact.

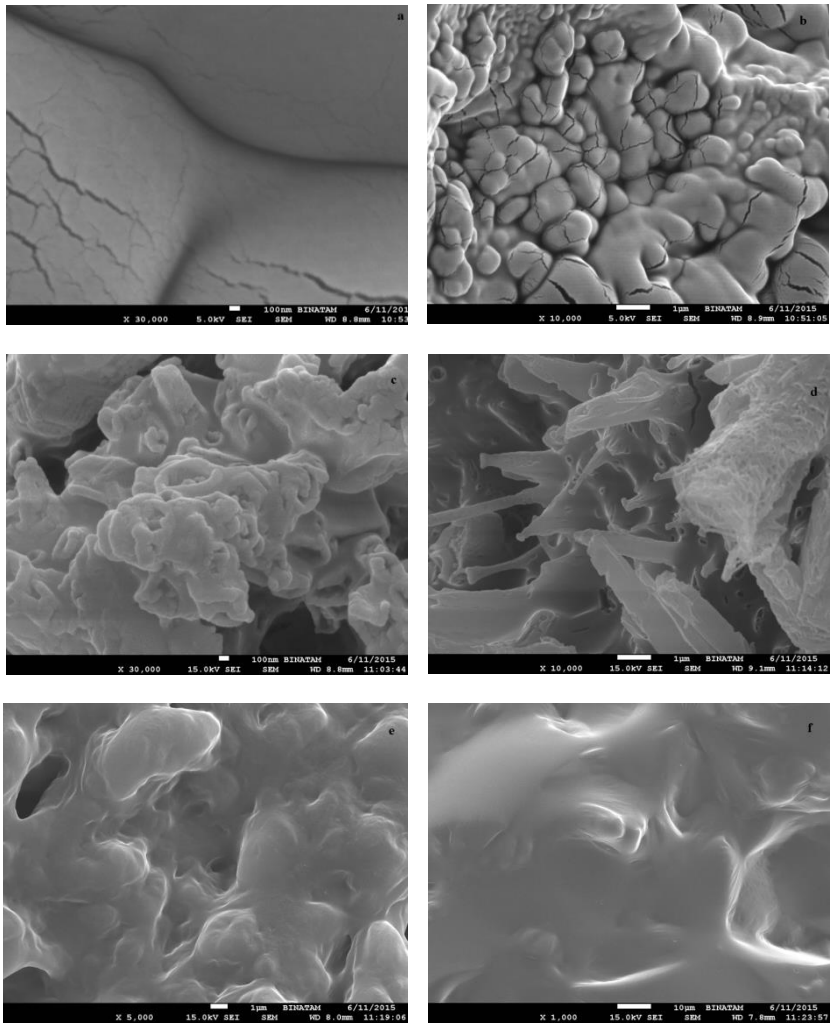

Figure 4.17 SEM images of (a-b) LiPVAOB-40PPEGMA, (c-d) LiOPAAB 20PPEGMA & (e-f) poly (AMPS-co-PEGMA)

4.5 IMPEDANCE SPECTROSCOPY

4.5.1 Conductivity of PVA-PPEGMA Composites

The ionic conductivity of lithium ion in PE's containing LIPVAOB-PPEGMA with different percentage of PPEGMA was measured by the ac impedance technique using equation 4.1

$$\sigma'(\omega) = \sigma_{ac}(\omega) = \varepsilon''(\omega)\,\omega\,\varepsilon_o \qquad (4.1)$$

Where $\sigma'(\omega)$ is the real part of the conductivity, $\omega = 2\pi f$ is the angular frequency, ε_o is the vacuum permittivity ($\varepsilon_o = 8.852\times10-14$ F/cm) and (ε'') is the imaginary part of the complex dielectric permittivity ($\varepsilon^*=\varepsilon'-i\varepsilon''$) [27, 37, 69]. The frequency dependence of the conductivity at various temperatures has been analyzed for all samples to get a better grasp of the ionic dynamics in the PE's. Figure 4.18-4.21 shows the frequency dependence of the ac conductivity (σ_{ac}) at various temperatures for LiPVAOB-XPPEGMA. In all polymer electrolyte samples ionic conductivity increases with elevation in temperature. As temperature elevates the movement of the ion becomes faster, causing an increase in ionic conduction [67].

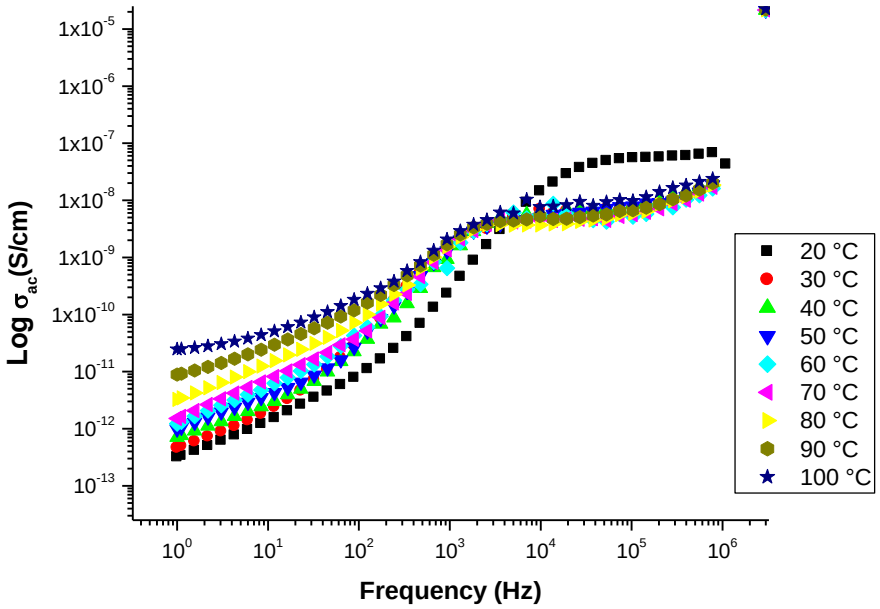

Figure 4.18 AC conductivity versus Frequency (Hz) of LiPVAOB at various temperatures

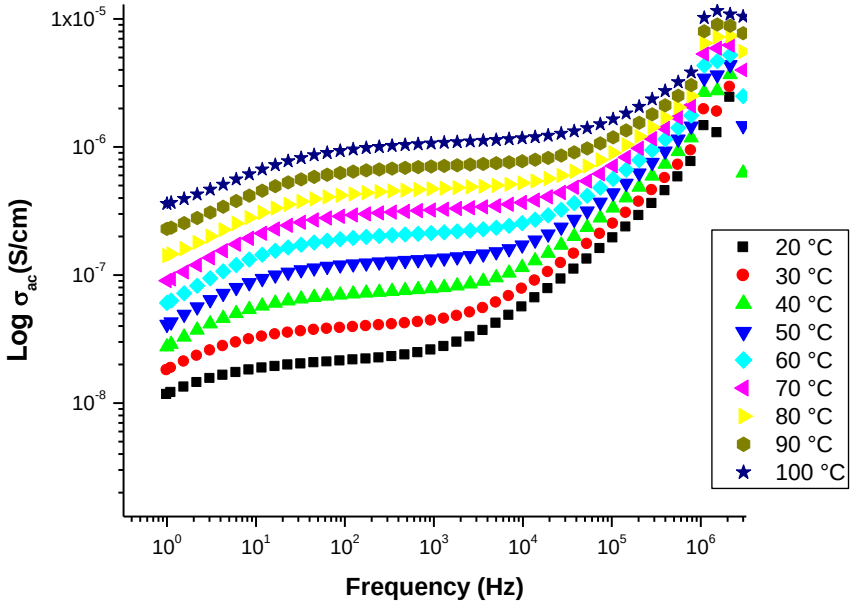

Figure 4.19 AC conductivity versus Frequency (Hz) of LiPVAOB-10PPEGMA at various temperatures

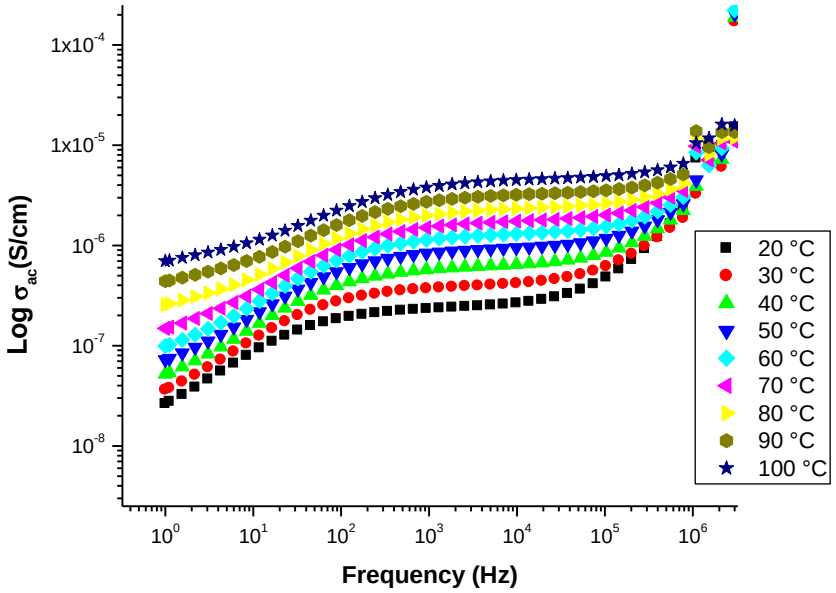

Figure 4.20 AC conductivity versus Frequency (Hz) of LiPVAOB-20PPEGMA at various temperatures

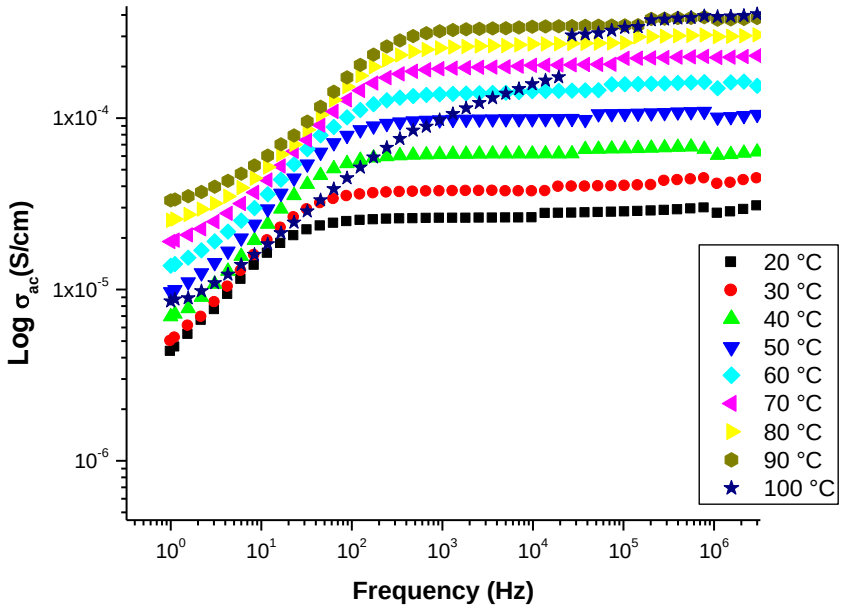

Figure 4.21 AC conductivity versus Frequency (Hz) of LiPVAOB-60PPEGMA at various temperatures

The DC conductivity (σ_{dc}) of the samples was obtained from the plateaus of log σ_{ac} versus log F by linear fitting of the data's. The conductivity isotherms are fitted in accordance to Arrhenius equation (equation 4.2) if the system follows tends to exhibit Arrhenius behaviour ;

$$\ln \sigma = \ln\sigma_o - E_a /kT \quad (4.2)$$

Where σ_o is the pre-exponential terms, E_a is the activation energy and k is the Boltzmann constant.

However if the system tends to behave in Vogel -Tamman- Fulcher (VTF) way then the DC conductivity curve is fitted accordance to VTF equation (equation 4.3) ;

$$\log \sigma = \log \sigma_o - E_v/[k(T-T_0)] \quad (4.3)$$

Where σ_o is the conductivity at the infinite temperature, E_v is the Vogel activation energy and T_0 the Vogel temperature [67].

Figure 4.22 represents the obtained σ_{dc} variation of the LiPVAOB-XPPEGMA as a function of the temperature, where the conductivity has been plotted as a function of 1000/T and is fitted according to Arrhenius equation due to its Arrhenius behavior. The conductivity isotherm illustrates that DC conductivity isotherm strongly depends on both the temperature and PPEGMA content.

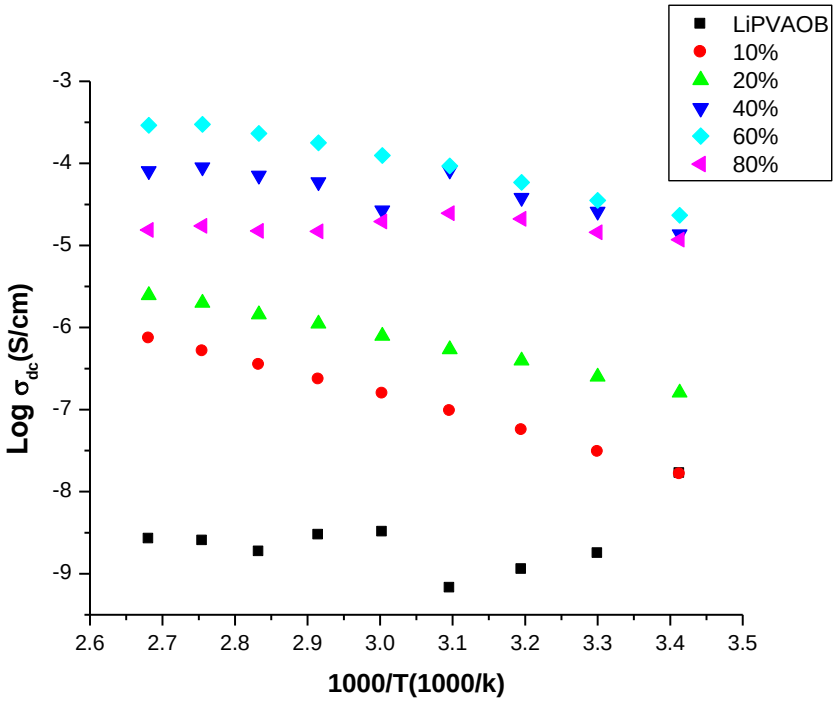

Figure 4.22 DC conductivities of LiPVAOB and LiPVAOB-XPPEGMA with X=10, 20, 40, 60 & 80

.

Ionic conductivity is achieved due to the mobility of the Li^+ ions. As seen in the figure the conductivity gradually increases with the elevated concentration of the PPEGMA in the PE's and reached a distinct maximum conductivity for LiPVAOB-60PPEGMA (i.e. $2.89 \times 10^{-4} S/cm^{-1}$ at 100ºC). With further addition of PPEGMA the conductivity seems to be falling. This behavior indicates the effect of segmental motion on the ionic conductivity since PPEGMA softens the material and its positive contribution on Li ion transport was previously reported. The decrease in conductivity with further PPEGMA addition is due to the decrease in Li ion concentration. Hence, LiPVAOB-60PPEGMA can be pronounced as the optimum sample for the following series. For all samples highest ionic conductivity was achieved at 100 ºC, which are summarized in Table 4.1

Table 4.1

Sample	% PPEGMA	Max Conductivity (S/cm) at 100 ºC	T_m/T_c (ºC)	Log σ_o	E_a (kJ/mol)
LiPVAOB-10PPEGMA	10	7.46×10^{-7}	118	-0.077	11.91
LiPVAOB-20PPEGMA	20	2.53×10^{-6}	118	-1.20	8.63
LiPVAOB-40PPEGMA	40	7.47×10^{-5}	118	-1.50	5.03
LiPVAOB-60PPEGMA	60	2.89×10^{-4}	147	0.85	8.48
LiPVAOB-80PPEGMA	80	1.37×10^{-5}	142	-4.60	0.27

4.5.2 Conductivity of PAA-PPEGMA Composites

Figure 4.23-4.25 shows the frequency dependence of the ac conductivity (σ_{ac}) at various temperatures for LiOPAAB-XPPEGMA. All sample exhibit higher conductivities at high temperature and frequency.

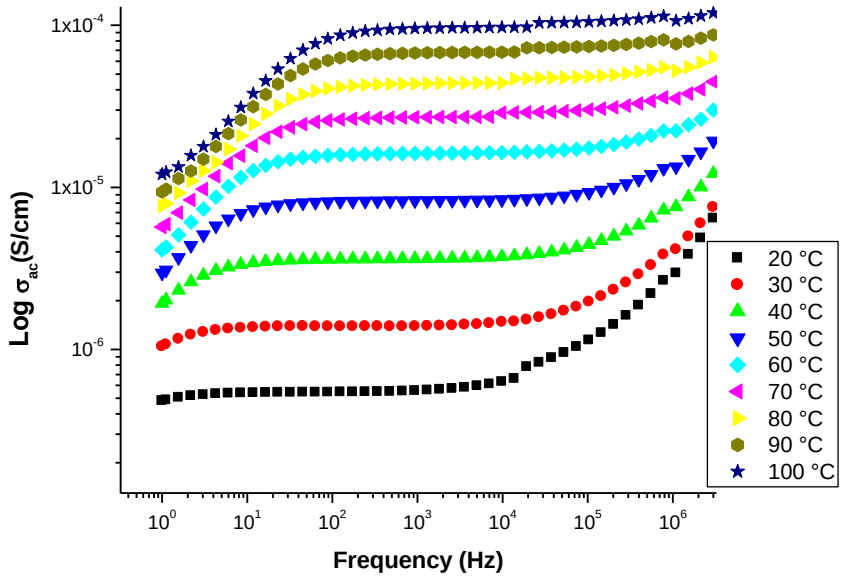

Figure 4.23 AC conductivity versus Frequency (Hz) of LiOPAAB-40PPEGMA at various temperatures

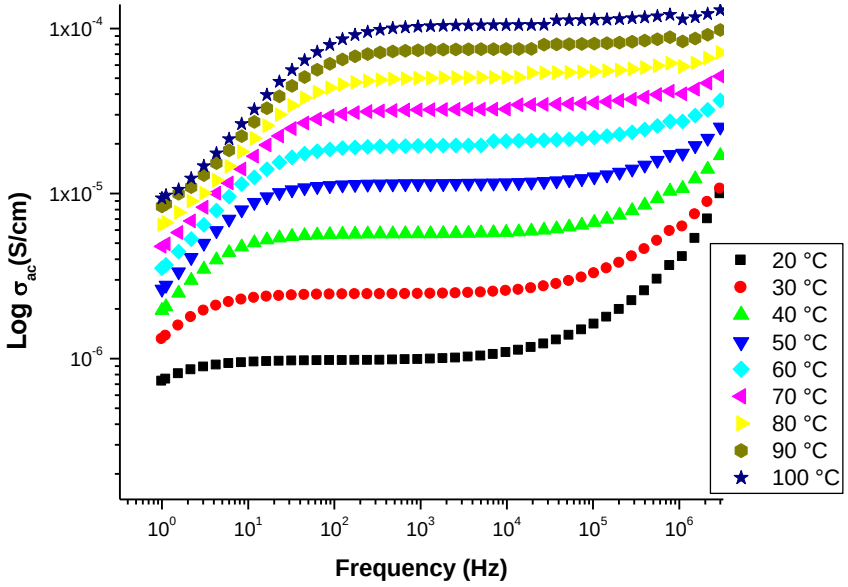

Figure 4.24 AC conductivity versus Frequency (Hz) of LiOPAAB-60PPEGMA at various temperatures

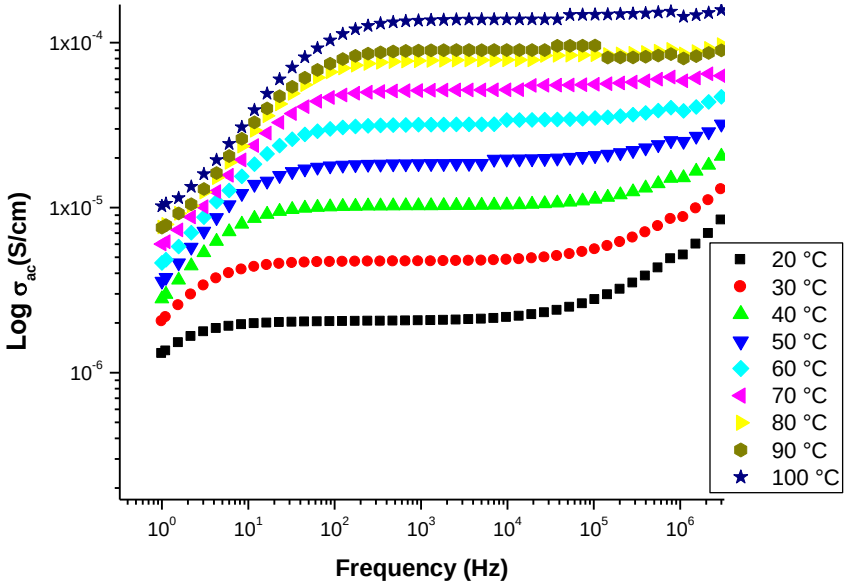

Figure 4.25 AC conductivity versus Frequency (Hz) of LiOPAAB-80PPEGMA at various temperatures

The DC conductivities of the PE samples were compared in Figure 4.26 to determine the effect of the PPEGMA on the conductivity. The graph indicates that the conductivity strongly depends on the temperature as well as on the concentration of PPEGMA. For LiOPAAB-XPPEGMA, the conductivity isotherm can be fitted according to Arrhenius equation (equation 4.2).

The ionic conductivity of the PAA-PPEGMA blends reaches a distinct maximum in conductivity when the concentration of PPEGMA is the highest. Similar to the previous section as the concentration of PPEGMA elevates the conductivity also elevates. However the conductivity of LiOPAAB-80PPEGMA, LiOBPAAB-60PPEGMA and LiOBPAAB-40PPEGMA are very close to each other, this might suggest that as PPEGMA ratio increases the conductivity starts to drop as well due the decrease in Li ion concentration. It is best to assume that beyond 80% PPEGMA the conductivity will drop further.

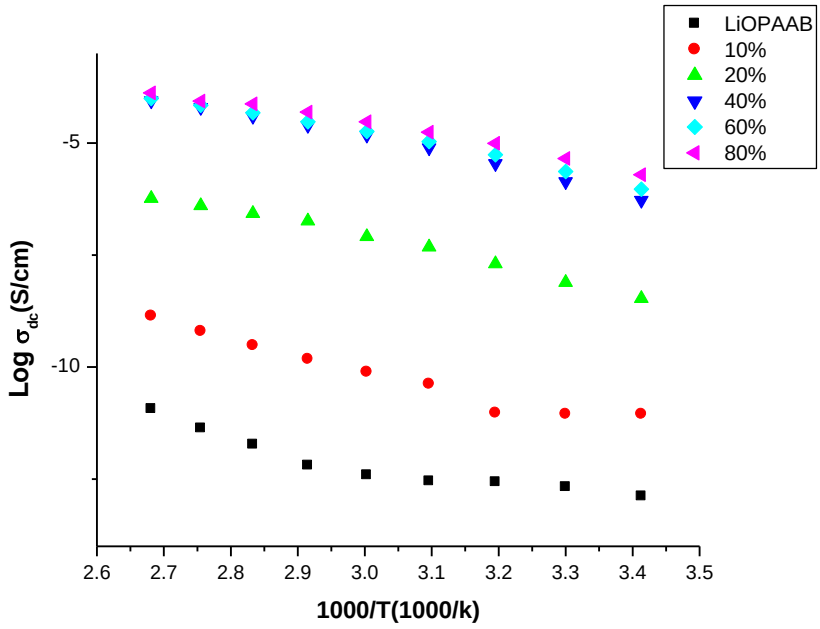

Figure 4.26 DC conductivities of LiOPAAB and LiOPAAB-XPPEGMA with X=10, 20, 40, 60 & 80

Table 4.2

Sample	% PPEGMA	Max Conductivity (S/cm) at 100 ºC	T_m /T_c (ºC)	Log σ_o	E_a (kJ/mol)
LiOPAAB - 10PPEGMA	10	7.21×10^{-8}	133	-0.34	17.12
LiOPAAB - 20PPEGMA	20	5.82×10^{-7}	88	2.21	16.50
LiOPAAB - 40PPEGMA	40	8.77×10^{-5}	89	4.18	16.00
LiOPAAB - 60PPEGMA	60	9.86×10^{-5}	91	3.40	14.30
LiOPAAB - 80PPEGMA	80	1.32×10^{-4}	92	2.80	13.20

4.5.3 Conductivity of PAMPS-PPEGMA Copolymer

Figure 4.27-4.28 shows the frequency dependence of the ac conductivity (σ_{ac}) at various temperatures for copolymer electrolytes. All sample exhibit higher conductivities at high temperature and frequency.

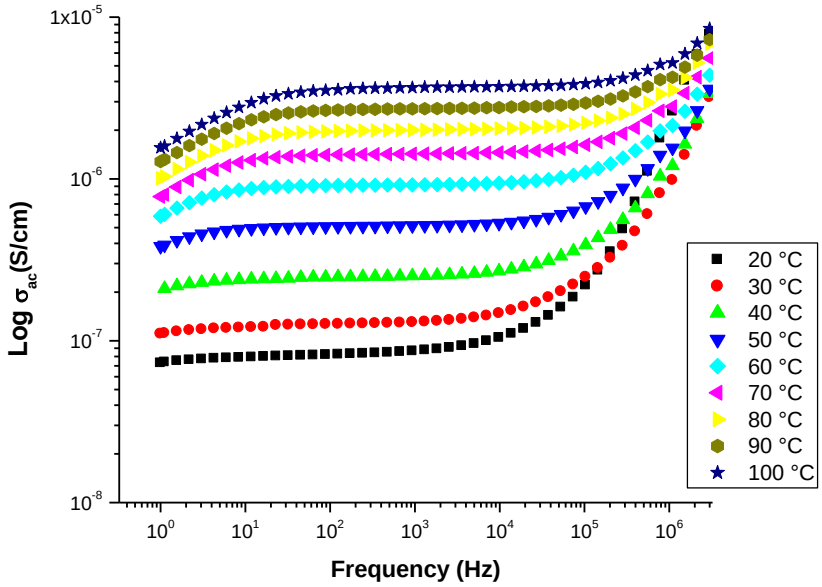

Figure 4.27 AC conductivity versus Frequency (Hz) of copolymer 1:1 at various temperatures

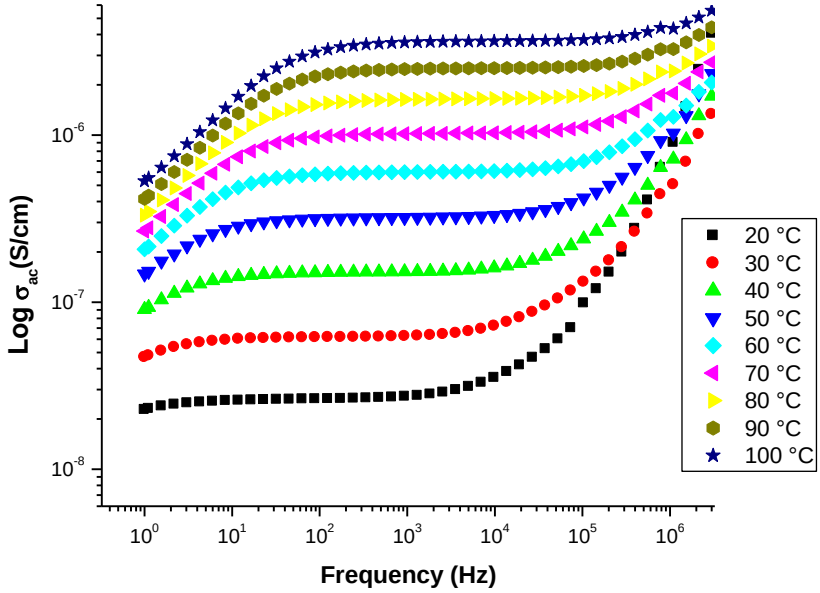

Figure 4.28 AC conductivity versus Frequency (Hz) of copolymer 1:2 at various temperatures

The DC conductivities of the copolymer electrolyte samples were compared in Figure 4.29 to determine the effect of PPEGMA on the conductivity. The graph indicates that the conductivity strongly depends on both temperature and PPEGMA content.

The conductivity gradually elevated with the elevated concentration of the PPEGMA in the PE's and reached a distinct maximum conductivity for copolymer ratio 1:1, similar to the previous section. The conductivity of 1:1 and 1:2 are very close to each other, this might suggest that as PPEGMA ratio increases the conductivity starts to drop as well. Just like the previous two studies, it is best to assume that beyond 80% PPEGMA the conductivity will drop further, due to the decrease in Li ion concentration.

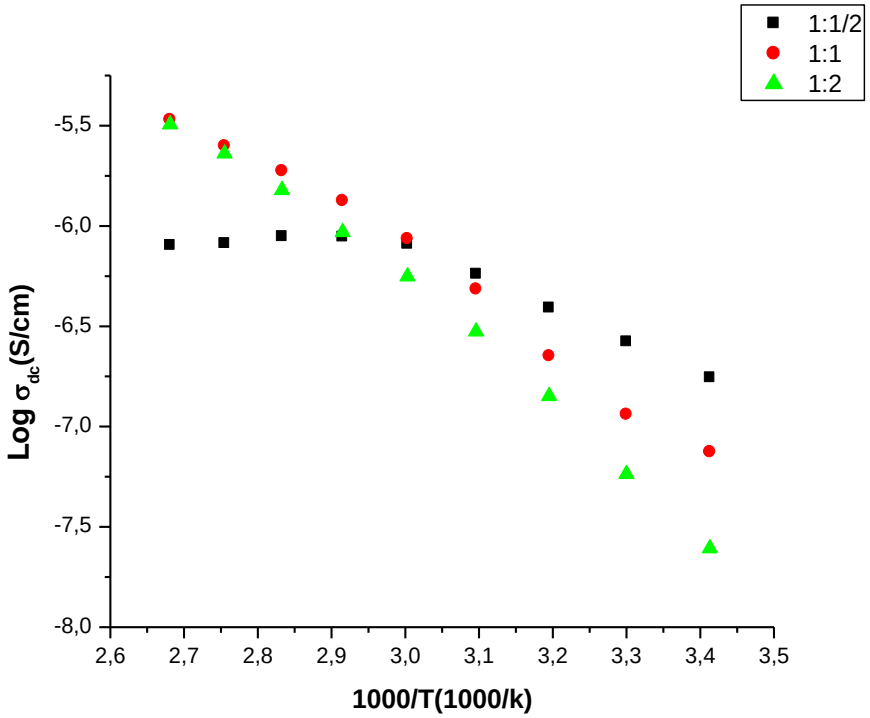

Figure 4.29 DC conductivities of copolymer electrolytes

Table 4.3

Sample	Mole ratio (AMPS:PEGMA)	Max Conductivity (S/cm) at 100 °C	T_g (°C)	Log σ_o	E_a (kJ/mol)
1:1/2	1:1/2	8.13×10^{-7}	102	-3.4	4.80
1:1	1:1	3.39×10^{-6}	89	0.98	12.70
1:2	1:2	3.22×10^{-6}	-	2.4	15.30

4.6 CYCLIC VOLTAMMETRY (CV)

Electrochemical stability deduced by CV is one of the most important criteria for energy storage devices such as the LIB's. CV was performed at room temperature as

demonstrated in Figure 4.30. The electrochemical stability range of the PAA based electrolytes was determined by running a potential sweep through the system stainless steel/solid electrolyte/Li, in the potential range where the redox reactions for the LIB's occur.

LiOPAAB-60PPEGMA displayed outstanding electrochemical stability window of approximately 4.5 V.

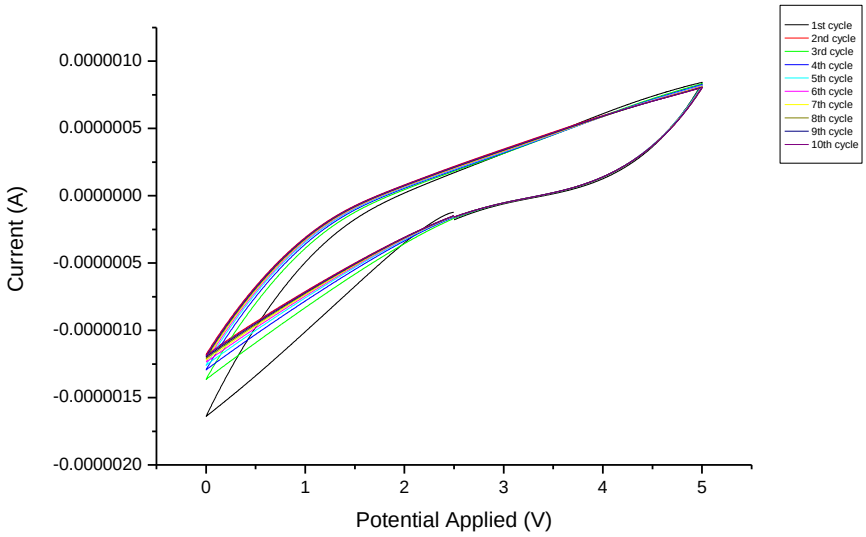

Figure 4.30 Cyclic voltammogram LiOPAAB-60PPEGMA electrolyte

CHAPTER 5

CONCLUSION

In the past couple of years several combinations of polymer and copolymer have been employed to produce PE's, which happen to be an excellent replacement for the conventional liquid electrolyte. Single ion systems may not reach such high conductivity but they tend to eliminate polarization side effects and have uniform transference increasing overall battery efficiency.

A novel single-ion conducting PE, LiPVAOB-XPPEGMA, on the groundwork of different molar ratios of PPEGMA was successfully synthesized. The successful formation of LiPVAOB and of the Li-complexes were verified by the means of FT-IR. TGA analysis showed the PE's were at least thermally stable up to 200 ºC. On the other hand DSC results suggested that the samples tend to lose crystallinity as the amount of PPEGMA increases. All the samples were homogeneous as suggested by SEM analysis. The ionic conductivity of the PE's increased with PPEGMA ratio as well as the temperature, which suggests Arrhenius behavior in all the PE's. The sample LiPVAOB-60PPEGMA showed highest conductivity of 2.89×10^{-4} S/cm at 100 ºC.

Novel LiOPAAB-XPPEGMA a single-ion conducting PE was successfully synthesized. Just like the previous work, FT-IR deduced the successful formation of LiOPAAB and of the Li-complexes. LiOPAAB-XPPEGMA PE's exhibited thermal stability up to 200 ºC as well. DSC illustrated homogeneity and amorphous characteristic, which increased as the amount of PPEGMA increases. Further homogeneity was confirmed by SEM analysis. All PE's displayed Arrhenius behavior, the ionic conductivity increased with increase in amount of PPEGMA and temperature. The sample LiPVAOB-80PPEGMA showed highest conductivity of 1.32×10^{-4} S/cm at

100 ºC. With CV it was verified that the PE's were electrochemically stable as well. The sample LiOPAAB-60PPEGMA displayed outstanding electrochemical stability window of approximately 4.5 V.

Novel poly (AMPS-co-PEGMA) was successfully synthesized by free radical polymerization. With FT-IR studies the formation of the copolymer and the Li-complexes were verified. The copolymers were stable thermally up to 200 ºC. Single T_g peaks in DSC verified the homogeneity and illustrated amorphous behavior. SEM analysis confirmed further homogeneity in all samples. The ionic conductivity in samples depends on both the amount of PPEGMA and the temperature, suggesting Arrhenius behavior. The sample poly (AMPS-co-PEGMA) (1:2) showed highest conductivity of 3.22×10^{-6} S/cm at 100 ºC.

The obtained electrolytes displayed both propitious thermal properties and morphology. The given electrolytes showed the highest conductivities up to 2.89×10^{-4} S/cm and are thermally stable at least up to 200 ºC. These PE's have reasonably high ionic conductivities and can be recommended for application to LIB's.

REFERENCES

[1] H. Aydın and A. Bozkurt, "Synthesis, characterization, and ionic conductivity of novel crosslinked polymer electrolytes for Li-ion batteries," *Journal of Applied Polymer Science,* vol. 124, pp. 1193-1199, 2012.

[2] J.-K. Park, *Principles and applications of lithium secondary batteries*: John Wiley & Sons, 2012.

[3] M. Winter and R. J. Brodd, "What Are Batteries, Fuel Cells, and Supercapacitors?," *Chemical Reviews,* vol. 104, pp. 4245-4269, 2004.

[4] R. Dell and D. A. J. Rand, *Understanding batteries*: Royal Society of Chemistry, 2001.

[5] C. Daniel and J. Besenhard, *Handbook of Battery Materials*: John Wiley & Sons, 2012.

[6] M. Root, *The TAB Battery Book: An In-depth Guide to Construction, Design, and Use*: McGraw Hill Professional, 2010.

[7] W. Van Schalkwijk and B. Scrosati, *Advances in lithium-ion batteries*: Springer Science & Business Media, 2002.

[8] G. R. Dahlin and K. E. Strøm, *Lithium Batteries: Research, Technology, and Applications*: Nova Science Publishers, 2010.

[9] V. Etacheri, R. Marom, R. Elazari, G. Salitra, and D. Aurbach, "Challenges in the development of advanced Li-ion batteries: a review," *Energy & Environmental Science,* vol. 4, pp. 3243-3262, 2011.

[10] R. Zhang, N. Hashemi, M. Ashuri, and R. Montazami, "Advanced gel polymer electrolyte for lithium-ion polymer batteries," in *ASME 2013 7th International Conference on Energy Sustainability collocated with the ASME 2013 Heat Transfer Summer Conference and the ASME 2013 11th International Conference on Fuel Cell Science, Engineering and Technology*, 2013, pp. V001T05A005-V001T05A005.

[11] R. Meziane, J.-P. Bonnet, M. Courty, K. Djellab, and M. Armand, "Single-ion polymer electrolytes based on a delocalized polyanion for lithium batteries," *Electrochimica Acta,* vol. 57, pp. 14-19, 2011.

[12] M. He, X. Zhang, K. Jiang, J. Wang, and Y. Wang, "Pure Inorganic Separator for Lithium Ion Batteries," *APPLIED MATERIALS & INTERFACES,* 2014.

[13] W. Xiao, L. Zhao, Y. Gong, J. Liu, and C. Yan, "Preparation and performance of poly (vinyl alcohol) porous separator for lithium-ion batteries," *Journal of Membrane Science,* vol. 487, pp. 221-228, 2015.

[14] P. Arora and Z. Zhang, "Battery separators," *Chemical Reviews,* vol. 104, pp. 4419-4462, 2004.

[15] L. Dai, *Intelligent macromolecules for smart devices: from materials synthesis to device applications*: Springer Science & Business Media, 2004.

[16] D. W. Bruce, D. O'Hare, and R. I. Walton, *Energy Materials*: John Wiley & Sons, 2011.

[17] H. Aydın and A. Bozkurt, "Synthesis, Characterization, and Ionic Conductivity of Novel Crosslinked Polymer Electrolytes for Li-Ion Batteries," 2011.

[18] S. Liang, U. H. Choi, W. Liu, J. Runt, and R. H. Colby, "Synthesis and Lithium Ion Conduction of Polysiloxane Single-Ion Conductors Containing Novel Weak-Binding Borates," *CHEMISTRY OF MATERIALS,* vol. 24, pp. 2316-2323, 2012.

[19] P. Carol, P. Ramakrishnan, B. Johna, and G. Cheruvally, "Preparation and characterization of electrospun poly(acrylonitrile) fibrous membrane based gel polymer electrolytes for lithium-ion batteries," *Journal of Power Sources,* vol. 196, pp. 10156-10162, 2011.

[20] B. K. Mandal, C. J. Walsh, T. Sooksimuang, and S. J. Behroozi, "New Class of Single-Ion-Conducting Solid Polymer Electrolytes Derived from Polyphenols," *CHEMISTRY OF MATERIALS,* vol. 12, 2000.

[21] A. Ramzy and V. Thangadurai, "Tailor-Made Development of Fast Li Ion Conducting Garnet-Like Solid Electrolytes," *APPLIED MATERIALS & INTERFACES,* vol. 2, pp. 385-390, 2010.

[22] R. J. Sengwa, P. Dhatarwal, and S. Choudhary, "Role of preparation methods on the structural and dielectricproperties of plasticized polymer blend electrolytes: Correlationbetween ionic conductivity and dielectric parameters," *Electrochimica Acta,* vol. 142, pp. 359-370, 2014.

[23] Z.-l. Wang and Z.-y. Tang, "A novel polymer electrolyte based on PMAML/PVDF-HFP blend," *Electrochimica Acta,* vol. 49, pp. 1063-1068, 2004. [24] Y. Xing, Y. Wu, H. Wang, G. Yang, W. Li, L. Xuc, and X. Jiang, "Preparation of hybrid polymer based on polyurethane lithium salt andpolyvinylidene fluoride as electrolyte for lithium-ion batteries," *Electrochimica Acta,* vol. 136, pp. 513-520, 2014.

[25] A. M. M. Ali, R. H. Y. Subban, H. Bahron, M. Z. A. Yahya, and A. S. Kamisan, "Investigation on modified natural rubber gel polymer electrolytes for lithium polymer battery," *Journal of Power Sources,* vol. 244, pp. 636-640, 2013.

[26] S. D. Tillmann, P. Isken, and A. Lex-Balducci, "Gel polymer electrolyte for lithium-ion batteries comprising cyclic carbonate moieties," *Journal of Power Sources,* vol. 271, pp. 239-244, 2014.

[27] S. Ü. Çelik and A. Bozkurt, "Polymer electrolytes based on the doped comb-branched copolymers for Li-ion batteries," *Solid State Ionics,* vol. 181, pp. 987-993, 2010.

[28] R. P. Doyle, X. Chen, M. Macrae, A. Srungavarapu, L. J. Smith, M. Gopinadhan, C. O. Osuji, and S. Granados-Focil, "Poly (ethylenimine)-Based Polymer Blends as Single-Ion Lithium Conductors," *Macromolecules,* vol. 47, pp. 3401-3408, 2014.

[29] J. Manuel, G. S. C. J.-H. Ahn, H.-S. Ryu, H.-J. Ahn, K.-W. Kim, and C. Nah, "Electrochemical performance of electrospun poly(vinylidene fluoride-co-hexafluoropropylene)-based nanocomposite polymer electrolytes incorporating ceramic fillers and room temperature ionic liquid," *Electrochimica Acta,* vol. 55, pp. 1347-1354, 2010.

[30] S. Feng, D. Shi, F. Liu, L. Zheng, J. Nie, W. Feng, X. Huang, M. Armand, and Z. Zhou, "Single lithium-ion conducting polymer electrolytes based on poly[(4-styrenesulfonyl)(trifluoromethanesulfonyl)imide] anions," *Electrochimica Acta,* vol. 93, pp. 254-263, 2013.

[31] Q. Lu, J. Fang, J. Yang, G. Yan, S. Liu, and J. Wang, "A novel solid composite polymer electrolyte based on poly(ethyleneoxide) segmented polysulfone copolymers for recharge able lithium batteries," *Journal of Membrane Science,* vol. 425-426, pp. 105-112, 2013.

[32] L. M. Bronstein, R. L. Karlinsey, B. Stein, Z. Yi, J. Carini, and J. W. Zwanziger, "Solid Polymer Single-Ion Conductors: Synthesis and Properties," *CHEMISTRY OF MATERIALS,* vol. 18, pp. 708-715, 2006.

[33] G. Derrien, J. Hassoun, S. Sacchetti, and S. Panero, "Nanocomposite PEO-based polymer electrolyte using a highly porous, super acid zirconia filler," *Solid State Ionics,* vol. 180, pp. 1267-1271, 2009.

[34] Q. Cheng, Z. Cui, J. Li, S. Qin, F. Yan, and J. Li, "Preparation and performance of polymer electrolyte based on poly(vinylidene fluoride)/polysulfone blend membrane via thermally induced phase separation process for lithium ion battery," *Journal of Power Sources,* vol. 266, pp. 401-413, 2014.

[35] M. Kurian, M. E. Galvin, P. E. Trapa, D. R. Sadoway, and A. M. Mayes, "Single-ion conducting polymer–silicate nanocomposite electrolytes for lithium battery applications," *Electrochimica Acta,* vol. 50, pp. 2125-2134, 2005.

[36] F. Lian, H.-y. Guan, Y. Wen, and X.-r. Pan, "Polyvinyl formal based single-ion conductor membranes as polymer electrolytes for lithium ion batteries," *Journal of Membrane Science,* vol. 469, pp. 67-72, 2014.

[37] S. Ü. Çelik and A. Bozkurt, "PEG crosslinked poly(vinylbenzene boronic acid) polymer electrolytes for Li-ion batteries," *Current Applied Physics,* vol. 13, pp. 1668-1673, 2013.

[38] A. Chandra, A. Chandra, and K. Thakur, "Synthesis, characterization and ion transport properties of hot-pressed solid polymer electrolytes (1− x) PEO: x KI," *Chinese Journal of Polymer Science,* vol. 31, pp. 302-308, 2013.

[39] K. E. Doan, M. A. Ratner, and D. F. Shriver, "Synthesis and Electrical Response of Single-Ion Conducting Network Polymers Based on Sodium Poly(tetraalkoxyaluminates," *CHEMISTRY OF MATERIALS,* vol. 3, pp. 418-423, 1991.

[40] M. L. Verma, M. Minakshi, and N. K. Singh, "Synthesis and characterization of solid polymer electrolyte based on activated carbon for solid state capacitor," *Electrochimica Acta,* vol. 137, pp. 497-503, 2014.

[41] N. Mobarak, A. Ahmad, M. Abdullah, N. Ramli, and M. Rahman, "Conductivity enhancement via chemical modification of chitosan based green polymer electrolyte," *Electrochimica Acta,* vol. 92, pp. 161-167, 2013.

[42] O. A. Ileperuma, G. A. Kumara, H.-S. Yang, and K. Murakami, "Quasi-solid electrolyte based on polyacrylonitrile for dye-sensitized solar cells," *Journal of Photochemistry and Photobiology A: Chemistry,* vol. 217, pp. 308-312, 2011.

[43] M. M. A. Khan, "PVC based polyvinyl alcohol zinc oxide composite membrane: Synthesis and electrochemical characterization for heavy metal ions," *Journal of Industrial and Engineering Chemistry,* vol. 19, pp. 1365-1370, 2013.

[44] A. Le Mehaute, G. Crepy, G. Marcellin, T. Hamaide, and A. Guyot, "Polymer electrolytes," *Polymer Bulletin,* vol. 14, pp. 233-237, 1985.

[45] G. Appetecchi, S. Scaccia, and S. Passerini, "Investigation on the Stability of the Lithium-Polymer Electrolyte Interface," *Journal of the Electrochemical Society,* vol. 147, pp. 4448-4452, 2000.

[46] H. Chen, J. Fergus, and C. Shannon, "Characterization of copolymer poly (acrylonitrile) based polymer electrolytes," *Journal of materials science letters,* vol. 21, pp. 285-287, 2002.

[47] S.-J. Park, A.-R. Han, J.-S. Shin, and S. Kim, "Influence of crystallinity on ion conductivity of PEO-based solid electrolytes for lithium batteries," *Macromolecular Research,* vol. 18, pp. 336-340, 2010.

[48] Y. S. Zhu, X. W. Gao, X. J. Wang, Y. Y. Hou, L. L. Liu, and Y. P. Wu, "A single-ion polymer electrolyte based on boronate for lithium ion batteries," *Electrochemistry Communications,* vol. 22, pp. 29-32, 2012.

[49] Y. S. Zhu, X. J. Wang, Y. Y. Hou, X. W. Gao, L. L. Liu, Y. P. Wu, and M. Shimizu, "A new single-ion polymer electrolyte based on polyvinyl alcohol for lithium ion batteries," *Electrochimica Acta,* vol. 87, pp. 113– 118, 2013.

[50] S. Guhathakurta and K. Min, "Lithium sulfonate promoted compatibilization in single ion conducting solid polymer electrolytes based on lithium salt of sulfonated polysulfone and polyether epoxy," *Polymer,* vol. 51, pp. 211-221, 2010.

[51] K. Sinha and J. Maranas, "Does Ion Aggregation Impact Polymer Dynamics and Conductivity in PEO-Based Single Ion Conductors?," *Macromolucules,* vol. 47, pp. 2718-2726, 2014.

[52] Y. Zhang, R. Rohan, W. Cai, G. Xu, Y. Sun, A. Lin, and H. Cheng, "Influence of Chemical Microstructure of Single-Ion Polymeric Electrolyte Membranes on Performance of Lithium-Ion Batteries," *APPLIED MATERIALS & INTERFACES,* vol. 6, pp. 17534-17542, 2014.

[53] R. Rohan, Y. Sun, W. Cai, Y. Zhang, K. Pareek, G. Xu, and H. Cheng, "Functionalized polystyrene based single ion conducting gel polymer electrolyte for lithium batteries," *Solid State Ionics,* 2014.

[54] P. V. Wright, "Developments in polymer electrolytes for lithium batteries," *Mrs Bulletin,* vol. 27, pp. 597-602, 2002.

[55] H. R. Allcock, D. T. Welna, and A. E. Maher, "Single ion conductors—polyphosphazenes with sulfonimide functional groups," *Solid State Ionics,* vol. 177, pp. 741-747, 2006.

[56] Y.-H. Liang, C.-C. Wang, and C.-Y. Chen, "Comb-like copolymer-based gel polymer electrolytes for lithium ion conductors," *Journal of Power Sources,* vol. 176, pp. 340-346, 2008.

[57] X.-G. Sun, J. Hou, and J. B. Kerr, "Comb-shaped single ion conductors based on polyacrylate ethers and lithium alkyl sulfonate," *Electrochimica Acta,* vol. 50, pp. 1139-1147, 2005.

[58] J. Cowie and G. Spence, "Novel single ion, comb-branched polymer electrolytes," *Solid State Ionics,* vol. 123, pp. 233-242, 1999.

[59] W. Li, Y. Xing, X. Xing, Y. Li, G. Yang, and L. Xu, "PVDF-based composite microporous gel polymer electrolytes containing a novelsingle ionic conductor SiO 2 (Li+)," *Electrochimica Acta,* vol. 112, pp. 183-190, 2013.

[60] F. Bertasi, K. Vezzù, G. A. Giffin, T. Nosach, P. Sideris, S. Greenbaum, M. Vittadello, and V. Di Noto, "Single-ion-conducting nanocomposite polymer

electrolytes based on PEG400 and anionic nanoparticles: Part 2. Electrical characterization," *International Journal of Hydrogen Energy,* vol. 39, pp. 2884-2895, 2014.

[61] M. Watanabe, Y. Suzuki, and A. Nishimoto, "Single ion conduction in polyether electrolytes alloyed with lithium salt of a perfluorinated polyimide," *Electrochimica Acta,* vol. 45, pp. 1187-1192, 2000.

[62] K. Matsushita, Y. Shimazaki, M. Mehta, and T. Fujinami, "Synthesis and characterization of aluminate polymer electrolytes and their blends with poly (ether) s," *Solid State Ionics,* vol. 133, pp. 295-301, 2000.

[63] X.-G. Sun, C. L. Reeder, and J. B. Kerr, "Synthesis and characterization of network type single ion conductors," *Macromolecules,* vol. 37, pp. 2219-2227, 2004.

[64] Y. Tominaga and H. Ohno, "Lithium ion conduction in linear-and network-type polymers of PEO/sulfonamide salt hybrid," *Electrochimica Acta,* vol. 45, pp. 3081-3086, 2000.

[65] K. Ito and H. Ohno, "Ionic conductivity of poly (ethylene oxide) having charges on the chain end," *Solid State Ionics,* vol. 79, pp. 300-305, 1995.

[66] H. Aydin, M. Senel, H. Erdemi, A. Baykal, M. Tulu, A. Ata, and A. Bozkurt, "Inorganic-organic polymer electrolytes based on poly(vinyl alcohol) and borane/poly(ethelene glycol) monomethyl ether for Li-ion battreies," *Journal of Power Sources,* vol. 196, pp. 1425-1432, 2011.

[67] M. Kaynak, A. Yusuf, H. Aydın, M. U. Taşkıran, and A. Bozkurt, "Enhanced ionic conductivity in borate ester plasticized Polyacrylonitrile electrolytes for lithium battery application," *Electrochimica Acta,* vol. 164, pp. 108-113, 2015.

[68] H. Erdemi, A. Bozkurt, and W. H. Meyer, "PAMPSA–IM based proton conducting polymer electrolytes," *Synthetic Metals,* vol. 143, pp. 133–138, 2004.

[69] S. Ü. Çelik and A. Bozkurt, "The synthesis and proton-conducting properties of the copolymers based on 1-vinyl-1,2,4-triazole and 2-acrylamido-2-methyl-1-propanesulfonic acid," *Solid State Ionics,* vol. 181, pp. 525–530, 2010.

[70] C. Ge, L. Wang, L. Xue, Z.-S. Wu, H. Li, Z. Gong, and X.-D. Zhang, "Synthesis of novel organic-ligand-doped sodium bis (oxalate)-borate complexes with tailored thermal stability and enhanced ion conductivity for sodium ion batteries," *Journal of Power Sources,* vol. 248, pp. 77-82, 2014.

[71] S. Günday, A. Bozkurt, W. H. Meyer, and G. Wegner, "Effects of different acid functional groups on proton conductivity of polymer-1, 2, 4-triazole blends," *Journal of Polymer Science Part B: Polymer Physics,* vol. 44, pp. 3315-3322, 2006.

[72] O. W. Guirguis and M. T. Moselhey, "Thermal and structural studies of poly (vinyl alcohol) and hydroxypropyl cellulose blends," 2011.

[73] W. Brostow, V. M. Castaño, A. Huanosta, M. de Icaza, and M. E. Nicho, "Poly (acrylic acid)+ zinc diacetate composites: High temperature service and electric conductivity," *Material Research Innovations,* vol. 3, pp. 85-91, 1999.